Exact solution of nanofluid flow over a stretching/shrinking sheet with dual availability

Thesis Submitted By

ZEESHAN ZAHOOR

01-248192-010

Supervised By

Dr. Rizwan ul Haq

A dissertation submitted to the Department of Computer Science, Bahria University, Islamabad as a partial fulfillment of the requirements for the award of the degree of MS

Session (2019 - 2021)

Bahria University
Discovering Knowledge

MS-13

Thesis Completion Certificate

Students' Name: **Zeeshan Zahoor** Registration Number: **66195**

Program of study: **MS (Mathematics)**

Thesis Title: **"Exact solution of nanofluid flow over a stretching/shrinking sheet with dual availability"**

It is to certify that the above student's thesis has been completed to my satisfaction and to my belief, its standard is appropriate for submission for Evaluation. I have also conducted plagiarism test of this thesis using HEC prescribed software and found similarity index at 15% that is within the permissible limit set by HEC for MS/MPhil degree thesis. I have also found the thesis in a format recognized by the BU for MS/MPhil thesis.

Principal Supervisor's signature: _____

Name: **Dr. Rizwan ul Haq** Date: **19-09-2021**

Bahria University
Discovering Knowledge

MS-14A

Author's Declaration

I, **Zeeshan Zahoor** here by state that my MS thesis Title **"Exact solution of nanofluid flow over a stretching/shrinking sheet with dual availability"** is my own work and has not been submitted previously by me for taking any degree from Bahria University or anywhere else in the country/world.

At any time if my statement is found to be incorrect even after my postgraduate, the university has the right to withdraw/cancel my MS degree.

Name of student: **Zeeshan Zahoor**

Date: **19-09-2021**

Bahria University
Discovering Knowledge

MS-14B

Plagiarism Undertaking

I, **Zeeshan Zahoor** solemnly declare that research work presented in the thesis titled **"Exact solution of nanofluid flow over a stretching/shrinking sheet with dual availability"** solely my research work with no significant contribution from any other person. Small contribution/help wherever taken has been duly acknowledge and that complete thesis has been written by me. I understand the zero-tolerance policy of the HEC and Bahria University towards plagiarism. Therefore, I as an author of the above title thesis declare that no portion of my thesis has been plagiarized and any material used as reference is properly referred/cited.

I undertake that if I am found guilty of any formal plagiarism in the above titled thesis even after award of MS degree, the university reserves the right to withdraw/revoke my MS degree and that HEC and the University has the right to publish my name on the HEC/University website on which names of students are placed who submitted plagiarized thesis.

Author's sign: _____

Name of student: **Zeeshan Zahoor**

Dedicated to

My beloved Mother

Whose prays and support have always been a source of inspiration. Although she is no longer in this world. Her suggestions and encouragement continue to regulate my life. Her sweet memories will remain forever in my heart. May ALLAH Almighty grant her high rank in Jannah, Ameen.

Acknowledgments

I am grateful to ALLAH Almighty for granting me to learn and attain benchmarks on the way to my aim, His beloved Prophet Hazrat **Muhammad** (ﷺ), who is a permanent source of guidance, knowledge, information and blessing for the whole creation. His instructions taught everyone how to live with pride, to stand with honor, and to be respectful.

My gratitude goes to my wonderful, hardworking, and extremely passionate supervisor Dr. Rizwan ul Haq, who has always been kind and supportive. His valuable expertise, comments, suggestions and instructions are most welcome that greatly improved the clarity of this thesis. Dr. Rizwan ul Haq has my sincere gratitude. I am so grateful to work under the supervision of such a great person.

I express my gratitude to my honorable professors who took me to the apex of my academia with their guidance. In particular, Prof. Dr. Muhammad Ramzan, Dr. Jafar Hasnain and Dr. Nazia Talat who have always been supportive in all of my course work and kept encouraging me throughout the session in Bahria University, Islamabad Campus. They are the true teachers who have made Mathematics Department of BUIC, a real place of learning.

My appreciation is to my family (especially my younger sister Nayab Zahoor) who always the real pillars of my encouragement showed their love, care and support throughout my life. Thank you for giving me strength to reach my goals and chase my dreams. As usual, so many friends and my class-mates have helped me throughout my MS that I cannot list them all. In particular, Dr. Syed Saqib Shah, Tabinda sajjad, Ali Raza, Syed Muhsin Aabas Naqvi, Robash Qasim, Sanaullah and Syed Hammad shah were specially remained enormously helpful throughout the period of my MS studies.

ZEESHAN ZAHOOR

Bahria University Islamabad, Pakistan

September, 2021

Contents

List of Figures

List of Tables

Nomenclature

V	velocity vector
T	fluid's temperature (K)
ρ_f	fluid's density (kgm^{-1})
$\tilde{u}, \tilde{v}$	velocity components (m/s)
μ_{nf}	nanofluids dynamic viscosity (kgm/s)
μ_f	dynamic viscosity (m^2/s)
ν_f	kinematic viscosity (m^2/s)
C_p	heat capacity $(Jkg^{-1}K^{-1})$
k_{nf}	thermal conductivity of nanofluid (W/Km)
$\bar{v}_w$	surface mass transfer
$\bar{h}_f$	heat transfer coefficient
M	magnetic parameter
k_f	thermal conductivity $(WK^{-1}m^{-1})$
$\bar{T}_\infty$	temperature at infinity
a, b, c	positive constant numbers
K	permeability of porous medium
R_f	thermal interfacial resistance
C_f	skin friction
Nu_x	local Nusselt number
$\bar{\tau}_w$	skin friction at wall
λ	stretching parameter
Pr	Prandtl number
Φ	porous medium parameter
Bi	Biot number
f_w	suction parameter
Ec	Eckert number
Re	Reynolds number
$\widehat{K}$	absorption co-efficient
ϕ	nanofluid volume fraction
q_r	radiative heat flux (Km^{-1})
$\widehat{\sigma}$	Stefan Boltzmann constant

Abstract

The present thesis determines the concept of the exact solution of nanofluid flow over a stretching/shrinking sheet with dual availability in the following steps. The thesis framework has been developed in the following way. In the first chapter, exhaustive literature is discussed for the exact solution of nanofluid flow across a stretching/shrinking sheet with dual availability. The precis details about nanofluids, boundary layer theory and heat transfer are discussed. Basic fluid terminologies and fundamental laws are explored in the second chapter. In third chapter, an article, closed solution of boundary layer flow on a moving surface embedded by nanofluid in the presence of magnetic field and suction/injection is reviewed. By using appropriate tensor, develop the continuity, energy and momentum equations. converted governing PDEs into dimensionless non-linear ODEs by adoption of favorable similarity variables and then solved analytically. In fourth chapter, extended the above mention work by applying porosity, thermal radiation and viscous dissipation to determine the dissipated energy during heat transfer. The consequences of porosity Φ, suction/injection f_w, stretching λ, and magnetic effect M on skin friction, velocity, temperature, and streamlines are well explored and showcased. An analysis of conclusions are included in fifth chapter.

Chapter 1

Introduction and literature review

Heat transfer is mandated in a broad range of technical applications, as well as in a huge number of industrial processes such as aircraft engine cooling,blow molding, temperature control etc. It is more efficient for heat transfer devices to transport a large quantity of heat across a small temperature difference when the temperature divergence is small. Energy consumption has emerged as a key element in the debate about the depletion of fossil fuel reserves. When heat is transferred through a fluid, this is known as convection. Many studies have been conducted to determine how to enhance the heat transfer and efficiency of fluids, thus reducing the amount of time needed for heat transfer to occur. Low thermal conductivity seems to be the most significant factor contributing to the low productivity of the heat exchanger in manufacturing sectors. The fact that a variety of techniques are used to enhance heat transfer is not without its limitations. Suspending small solid particles in fluids is a novel technique of increasing their thermal conductivity by increasing their surface area. Slurry may be created by mixing a variety of granules into a fluid, including metallic, non-metallic, and polyethylene particles, among other materials. It is expected that the thermal conductivity of aerosols in fluids will be higher than that of normal fluids. All prior study on suspension thermal conductivity, on the other hand, has been confined to millimeter-scale measurements. It is widely known that the thermal conductivity of suspensions goes up with the tiny particle's surface area to volume fraction. *Choi* [1] had been the earliest to offer up the core idea of nanofluid, which is a kind of fluid that contains embedded nanoparticles. Nanofluids are a fantastic alternative to traditional thermal systems in a wide range of applications. The fluid in which nano-sized particles with lengths

ranging from 1-100nm are suspended is referred to as nanofluid. Nanofluids have enough potential to boost the thermal conductivity of a base fluid, while nanoparticles have a higher capability to improve heat transfer than either. Nanofluids are used in a wide range of applications [2] in electronics, automobiles, and nuclear technology, in which efficient heat dissipation and enhanced heat transmission are necessary. After that,*Lixing cheg* [3] briefly highlights the advancements in nanofluid technology. Latterly *Yang et al* [4] investigated the thermal characteristics of linear motion of nanofluids. In the view of *Tiwari and Das* [5], a nanofluid theory focusing on the particle volume fraction was given to them. There have been a large number of researchers that have focused on improving heat transmission by utilizing nanofluids [6–11].

Thin layer of flowing viscous fluid near to the surface is known as boundary layer. It has huge assortment of applications like aerospace, sport aerodynamic, heat transfer enrichment, moving lids etc. *Prandtl* [12] was the earliest researcher who developed the theory of boundary layer. In research, he discussed the flow field and separated it into two portions. The first one is an inside boundary layer, where velocity gradient occurs, and second one is outer side of boundary layer, where viscosity can be ignored. Many researchers attempted to discover a closed solution but were unable to find solution, thus the approximation is still commonly used. Later, in 1961, *Sakiadis* [13] was the first to explore boundary layer flow over a solid surface using constant velocity. He used both close and approximate approaches to examine the solution of boundary layer. He was consequently unable to provide the exact solution for above mention model. After the research of Prandtl, when the transverse velocity component at the surface of plate is nonzero, a moving continuous flat plate is considered by *Erickson* [14]. Subsequently *Crane* [15]

studied the boundary layer flow on an expanding (stretched) sheet in 1970. He developed an exact solution for steady, 2-D, in-compressible boundary layer flow when the velocity is fluctuating. *Gupta and Gupta* [16] extended the work of Erickson by considered suction/injection. An exact solution of temperature distribution developed by *Grubka and Bobba* [17] using Kummer's function. *Banks* [18] worked on the field flow of extended (stretched) surface and variable velocity with power law. An extended work further by *Ali* [19] and *elbashbeshy* [20] on the porous stretching surface. *Miklavcic* [21] and *Wang* [22] studied the fluid motion caused by extending (stretching) the surface in two directions. Later on, many other researchers worked on the boundary layer due to shrinking/stretching surfaces [23–25].

Thermal radiation is said to be the procedure in which a heated surface emits energy in the form of electromagnetic radiation throughout all directions. Radiation is the process through which energy is transmitted across material in the form of waves or particles. Radiation is classified into three types: sound, energy, and light. Thermal radiations are employed to calculate energy transfer in the production of polymers and fossil fuels, as well as in astrophysical fluxes. Thermal radiation is essential in space exploration, high-temperature operations, and regulating the heating process within that polymer industrial sector, among other applications.

Brownian motion was discovered as the primary mechanism behind nanofluids that boost thermal conductivity. It has been founded that nanoparticles with smaller sizes can improve the thermal conductivity at elevated temperatures than nanoparticles with larger diameters. The literature has a variety of models, each of which emphasizes a particular process as the primary mechanism, such as Brownian motion or liquid layering. Recently, researchers examined the two components of effective thermal conductivity, namely the

static and dynamic components, as suggested by Koo, Kleinstreuer and Li (KKL) [27, 28]. Later *Sheikholeslami* [29] and many other researchers used the KKL models in there recent develop models [30–32].

Recently *Khan et al* [33] is endeavored to examine solution of dual nature of heat exchange and fluid flow on shrinking/stretching sheet. *Haq et al* [34–36]also worked on dual nature solution.

Our goal is to use of KKL model to examine dual availability of solution for nanofluid flow shrinking sheet underneath magnetic field action, this work is motivated by that of the existing literature. Thermal radiation effect is used with the saturation of nanoparticles within the base fluid (water). Viscous dissipation is also considered to determine dissipated energy during convective heat transfer. Dual solutions have been found for velocity and temperature. An analysis of conclusions are included in the last chapter.

Chapter 2

Basic definitions and concepts

In this chapter, several basic concepts, definition and laws related to fluid flow and heat transfer are being briefly addressed.

2.1 Fluid

The matter has three types solid, liquid and gases. The combination of liquid and gases is called fluid.

2.2 Fluid mechanics

The branch of mechanics concerned itself with the characteristics of fluids in motion or at rest. It is split into three parts. static fluid, fluid dynamics and kinematics.

2.2.1 Statics fluid

The investigation of fluid particles at rest is termed as statics fluid.

2.2.2 Fluid dynamics

Fluid dynamics is the analysis of the motion of the particles contained in a fluid.

2.2.3 Fluid kinematics

Fluid kinematics is the examination of the movement of fluid particles in the absence of any extraneous force.

2.3 Properties of fluid

2.3.1 Kinematic viscosity

The fractional relation of dynamic viscosity to density is characterized as termed kinematics viscosity. It is denoted by ν. Mathematically kinematic viscosity is expressed as

$$\nu = \frac{dynamic\ viscosity}{density} = \frac{\mu}{\rho}$$

.

2.3.2 Dynamic viscosity

Dynamic viscosity is identified fractional connection of shear stress to deformation rate, that's denoted by μ. Mathematically,

$$\mu = \frac{shear\ stress}{deformation\ rate}$$

Its dimension $[L^2T^{-1}]$.

2.3.3 Density

The density of a fluid's particle is defined as the ratio of its mass to its volume, and it is represented as ρ. Mathematically,

$$\rho = \frac{m}{V}$$

Dimension is $[ML^{-3}]$.

2.4 Classification of fluid

2.4.1 Ideal fluid

Ideal fluid (inviscid fluid)is defined as fluid with zero viscosity.

2.4.2 Real fluid

The fluid with viscosity which is not at zero, is called real fluid.

2.4.3 Compressible fluid

When the density of fluid directly proportional to the temperature and pressure, referred compressible fluid.. One of most common example is of gases.

2.4.4 Incompressible fluid

If density remains constant regardless of the temperature and pressure,such fluid is known as incompressible fluid. In general, liquids are considered to be incompressible.

2.5 Two-Dimensional flow

Dimensions are basically the space coordinates and mostly the fluid motions are considered to be three dimensional but for the convenience in its calculation, it is taken to be two dimensional so that it can easily be dealt with. 2-D flow means flow to be in the plane coordinate.

2.6 Boundary layer

Thin layer of a flowing viscous fluid nearest to the surface is boundary layer. It has large assortment of applications like aerospace,sport aerodynamic, heat transfer enhancement,polymer extrusion and so on.

2.7 Convection

When a heated fluid, such as air or water, moves across a space, heat is transmitted via that fluid. Convection occurs as a consequence of the propensity among most fluids to expand when they heat up.

2.8 Porous medium

Porous media are those that have tiny openings in their surface that enable fluids to flow through them. Porous-surfaced items contain vacuum areas or pores by which fluid particles may pass. Wooden materials, sand, tissue papers, sponges and foams are examples of porous medium.

2.9 Nanofluids

The fluid in which nano-sized particles with 1-100nm length are suspended is called nanofluid. Nanofluids have capable ability to boost the thermal conductivity of base fluid, Nanoparticles have greater potential to enhance heat transfer.

2.10 Heat and mass transfer

Heat transfer is a kinetic process in which energy is transferred from one particle to another via the movement of particles. Mass transfer, on the other hand, is the movement of mass from one location to another, as in absorption, evaporation, and so on.

2.11 Thermal radiation

Thermal radiation is said to be the procedure in which a heated surface emits energy in the form of electromagnetic radiation throughout all directions. Radiation is the process through which energy is transmitted across material in the form of waves or particles.

2.12 Hypergeometric confluent function

A confluent hypergeometric function is a solution to a confluent hypergeometric equation, which is a degenerate version of a hypergeometric differential equation in which two of the three regular singularities combine to produce an irregular singularity.

2.12.1 Kummer's function

Kummer's (confluent hypergeometric) function $M(a, b, z)$, introduced by Kummer (1837), is a solution to Kummer's differential equation. This is also known as the confluent hypergeometric function of the first kind.
Kummer's equation may be written as:

$$z\frac{d^2w}{dz^2} + (b - z)\frac{dw}{dz} - aw = 0,$$

with a regular singular point at $z = 0$ and an irregular singular point at $z = \infty$. It has two (usually) linearly independent solutions $M(a, b, z)$ and $U(a, b, z)$. Kummer's function of the first kind M is a generalized hypergeometric series given by:

$$M(a, b, z) = \sum_{n=0}^{\infty} \frac{a^{(n)} z^n}{b^{(n)} n!} = |F|(a; b; z),$$

where:

$$a^{(0)} = 1,$$

$$a^{(n)} = a(a + 1)(a + 2) \cdots (a + n - 1)\,,$$

is the rising factorial.

2.13 Some useful non-dimensional numbers

2.13.1 Reynolds number

The non-dimensional number defining the change in the inertial forces to the viscous forces. Mathematically;

$$Re = \frac{ax^2}{\nu}$$

2.13.2 Prandtl number

It is the non-dimensional number which is a change in kinematic viscosity ν with respect to thermal diffusivity λ. Mathematically,

$$Pr = \frac{\nu}{\lambda}$$

2.13.3 Biot number

It is a non-dimensional number defined as, When the heat transfer coefficient is being multiplied with the characteristic length and divided with thermal conductivity of the body. Generally, it can be expressed as;

$$Bi = \frac{L_c h}{k}$$

Here $L_c = \frac{Volume\ of\ body}{surface\ area}$, characteristic length, h is heat transfer coefficient and k is thermal conductivity.

2.13.4 Eckert number

The fractional relation of kinetic energy and enthalpy is characterized termed Eckert number. Generally, it can be expressed as;

$$Ec = \frac{advective\ mass\ transfer}{viscous\ dissipation}$$

2.13.5 Nusselt number

A dimensionless number which is the ratio between the convective and the conductive heat transfer at the boundary is called local Nusselt number. Mathematically, it is expressed as;

$$Nu_x = \frac{xh_x}{k}$$

Chapter 3

A closed solution of boundary layer flow on a moving surface enclosed by nanofluid in the presence of magnetic field and suction/injection

The main objective of this chapter is to investigate flow of boundary layer and heat transfer over moving surface in the presence of magnetic field and suction/injection. Initially, governing equations are formulated. Later on, with the help of similarity variables, transformed the governed nonlinear PDEs to the dimensionless nonlinear ODEs to obtain closed form solution of momentum and energy. The presence of some other parameters on energy and momentum equations can also be seen. This chapter is the review of [26].

3.1 Formulation of the problem

Consider the laminar, 2-D and steady flow of viscous nanofluid on a continuous moving surface. By assuming surface velocity U_w and mass transfer velocity V_w. Let magnetic field effect β_0 be the normal to the surface. Considering water as base fluid contains either Silver or Copper or Aluminum oxide. All nanoparticles are considered to be of the same size. In addition, suppose that the fluids phases and nanoparticles are in thermally equilibrium and there is no slip between both fluids. The governing equations of boundary layer for 2-D laminar steady nanofluid flows on moving surface are;

$$\nabla \cdot V = 0, \tag{3.1}$$

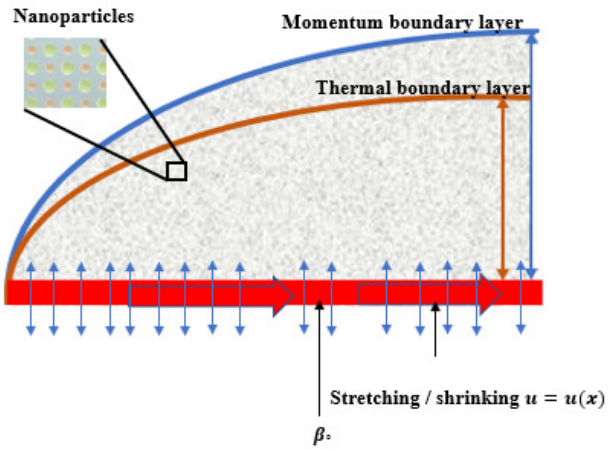

Fig. 1: Geometry of the problem

$$\rho_{nf}(V \cdot \nabla)V = div\tau - \sigma\beta_0^2 V, \tag{3.2}$$

$$(\rho C_p)_{nf}(V \cdot \nabla)T = \tau \cdot (\nabla V) - divq_c, \tag{3.3}$$

Here, τ can be expressed as;

$$\tau = -pI + \mu R_1, \tag{3.4}$$

R_1 is first Rivlin-Ericksen tensor, that is,

$$R_1 = (\nabla V) + (\nabla V)^T, \tag{3.5}$$

$$\nabla V = gradV, \tag{3.6}$$

$$q_c = -k\ (\nabla T), \tag{3.7}$$

For given problem, we define

the velocity field as $V = [\tilde{u}(x, y), \tilde{v}(x, y), 0]$,

and temperature

$$T = T(x, y), \tag{3.8}$$

Using Eq. (3.8) in Eqs. (3.5) and (3.6), we get

$$\nabla V = \begin{pmatrix} \tilde{u}_x & \tilde{u}_y & 0 \\ \tilde{v}_x & \tilde{v}_y & 0 \\ 0 & 0 & 0 \end{pmatrix} \text{ and } (\nabla V)^T = \begin{pmatrix} \tilde{u}_x & \tilde{v}_x & 0 \\ \tilde{u}_y & \tilde{v}_y & 0 \\ 0 & 0 & 0 \end{pmatrix}, \quad (3.9)$$

Now, by utilizing Eq. (3.9) in Eq. (3.5), we obtain

$$E_1 = \begin{pmatrix} 2\tilde{u}_x & (\tilde{u}_y + \tilde{v}_x) & 0 \\ (\tilde{v}_x + \tilde{u}_y) & 2\tilde{v}_y & 0 \\ 0 & 0 & 0 \end{pmatrix}, \quad (3.10)$$

Substituting Eq. (3.10) in Eq. (3.4), it results

$$\tau = \begin{pmatrix} -p + 2\mu(\tilde{u}_x) & \mu(\tilde{u}_y + \tilde{v}_x) & 0 \\ \mu(\tilde{v}_x + \tilde{u}_y) & -p + 2\mu\tilde{v}_y & 0 \\ 0 & 0 & -p \end{pmatrix}, \quad (3.11)$$

To express the matrix Eq. (3.11) in component form, we have

$$\tau_{xx} = -p + 2\mu(\tilde{u}_x), \quad \tau_{xy} = \tau_{yx} = \mu(\tilde{v}_x + \tilde{u}_y), \quad (3.12)$$

$$\tau_{xz} = \tau_{zx} = \tau_{yz} = \tau_{zy} = 0, \quad \tau_{yy} = -p + 2\mu(\tilde{v}_y), \quad (3.13)$$

$$\tau_{zz} = -p, \quad (3.14)$$

Using Eqs. (3.12), (3.13) and (3.14) in Eq. (3.2), we get

$$\rho(\tilde{u}\tilde{u}_x + \tilde{v}\tilde{u}_y) = -\frac{\partial p}{\partial x} + \mu\nabla^2\tilde{u} - \sigma\beta_0^2\tilde{u}, \quad (3.15)$$

$$\rho(\tilde{u}\tilde{v}_x + \tilde{v}\tilde{v}_y) = -\frac{\partial p}{\partial y} + \mu\nabla^2\tilde{v} - \sigma\beta_0^2\tilde{v}, \quad (3.16)$$

$$0 = -\frac{\partial p}{\partial z}, \tag{3.17}$$

In the Eq. (3.3), $\tau \cdot (\nabla V)$ be zero due to the absence of viscous dissipation and q_c from Eq. (3.7) gives;

$$\tau \cdot (\nabla V) = 0, \tag{3.18}$$

$$q_c = -k\ [T_x\ ,\ T_y\ ,\ 0], \tag{3.19}$$

Now, utilizing the above equations Eqs. (3.18) and (3.19) in Eq. (3.3), we obtain

$$\rho C_p\ (\tilde{u}T_x + \tilde{v}T_y) = k_{nf}\nabla^2 T, \tag{3.20}$$

The boundary conditions of the preceding problem would be as follows

$$\tilde{u} = \tilde{u}_w(x) = ax, \quad \tilde{v} = \tilde{v}_w \quad \text{at} \quad y = 0, \tag{3.21}$$

$$\tilde{u}(y\ \rightarrow\ \infty)\ \rightarrow\ 0. \tag{3.22}$$

Here, $\tilde{v}_w$, mass transfer on the surface for suction velocity ($\tilde{v}_w < 0$) and injection velocity ($\tilde{v}_w > 0$).

$$T = \bar{T}_w = \bar{T}_\infty + bx \qquad \text{at} \qquad y = 0, \tag{3.23}$$

$$T(y\ \rightarrow\ \infty)\ \rightarrow\ \bar{T}_\infty\ . \tag{3.24}$$

C_f and Nu_x can be written as

$$C_f = \frac{\bar{\tau}_w}{\rho \tilde{u}_w^2}\ , \qquad Nu_x = \frac{x\bar{q}_w}{k_{nf}(\bar{T}_w - \tilde{T}_\infty)}, \tag{3.25}$$

$$\bar{\tau}_w = \mu(\tilde{u}_y)\ , \quad \bar{q}_w = -k_{nf}(T_y) \quad \text{at} \quad y\ =\ 0. \tag{3.26}$$

We look for similarity equation, of the nonlinear PDEs (3.15, 3.16, 3.20)

Table 1: Thermal properties of Cu and water

Physical properties	**Base fluid (water)**	Cu
C_p(J/kgK)	4179	385
ρ(kg/m^3)	997.1	8933
k(W/mK)	0.613	400
$\alpha \times 10^7$ (m/s)	1.47	1163.1

to dimensionless nonlinear ODEs by introducing similarity variables as

$$\eta = y\sqrt{\frac{a}{\nu}}, \quad \psi = \sqrt{a\nu}xf(\eta), \quad \theta(\eta) = \frac{T - \bar{T}_\infty}{\bar{T}_w - \bar{T}_\infty}, \tag{3.27}$$

Converting ψ into $\tilde{u}$ and $\tilde{v}$, we get

$$\tilde{u} = axf'(\eta), \quad \tilde{v} = -\sqrt{a\nu}f(\eta). \tag{3.28}$$

Here, prime symbolizes the differentiation of a function w.r.t. η. By applying the above similarity transformations Eq. (3.27) on Eqs. (3.15), (3.16) and (3.20), we obtain the dimensionless ODE as

$$f'''+B(1-\phi)^{2.5}(ff''-f'^2)-M(1-\phi)^{2.5}f' = 0\,, \tag{3.29}$$

$$\theta''+\frac{Pr}{L}(f\theta'-f'\theta) = 0\,, \tag{3.30}$$

The reduced boundary conditions are

$$f(0) = f_w\,,\ f'(\infty) = 0\,,\ f'(0) = 1, \tag{3.31}$$

$$\theta(0) = 1\,,\ \theta(\infty) = 0\,. \tag{3.32}$$

Where, M is magnetic parameter, Pr is the prandtl number and f_w is section/injection.

$$Pr = (\frac{\nu\rho Cp}{k})_f,\ M = \frac{\sigma\beta_0^2}{a\rho_f}, B = (1-\phi+\phi\frac{\rho_s}{\rho_f}),\ L = \frac{\frac{k_{nf}}{k_f}}{1-\phi+\phi\frac{(\rho Cp)_s}{(\rho Cp)_f}}\ , \tag{3.33}$$

Also, using Eq. (3.27) in Eqs. (3.25) and (3.26), we get

$$C_f = \frac{2\tau_w}{U_w^2} = \frac{-2m}{\sqrt{Re}(1-\phi)^{2.5}}\ \ , \tag{3.34}$$

where, $Re_x = (ax^2/\nu)$, local Reynolds number,

$$Nu_x = \frac{xq_W}{k_f(T_w - T_\infty)} = -\frac{k_{nf}}{k_f}\ (Re)\theta'(0)\ , \tag{3.35}$$

where $q_w = -k_{nf}(\frac{\partial T}{\partial y})_{y=0} = -k_{nf}(T_w - T_\infty)\sqrt{\frac{a}{\nu_f}}\ \theta'(0)$.

To establish the solution of the transformed dimensionless nonlinear ODEs, assume the solution of Eq. (3.29) satisfying boundary conditions as

$$f(\eta) = f_w + \frac{1}{m}(1-e^{-m\eta})\ , \tag{3.36}$$

Using Eq. (3.36) in Eq. (3.29), it yields

$$m^2 - B(1-\phi)^{2.5} f_w m - (B+M)(1-\phi)^{2.5} = 0\ , \tag{3.37}$$

Solving the above equation for the value of m, we get

$$m = \frac{1}{2}(f_w B(1-\phi)^{2.5} + \sqrt{(f_w B(1-\phi)^{2.5})^2 + 4(B+M)(1-\phi)^{2.5}}),$$

(3.38)

Eq. (3.38) shows solution of the given problem. From Eqs. (3.28) and (3.36), we obtain

$$\tilde{u} = axe^{-m\eta} \quad \text{and} \quad \tilde{v} = -\sqrt{a\nu}(f_w + \tfrac{1}{m}(1-e^{-m\eta})). \tag{3.39}$$

In order to get the solution of the energy equation in the form of non-dimensional nonlinear ODE, we consider a new variable ξ as follows:

$$\xi = \frac{Pr}{Lm^2} e^{-m\eta} \ , \tag{3.40}$$

To apply this variable in Eq. (3.30), we convert the differentiation w.r.t η by using chain rule for first and second order ODEs, that is,

$$\tfrac{d}{d\eta} = \tfrac{d}{d\xi} \cdot \tfrac{d\xi}{d\eta} \quad \text{and} \quad \tfrac{d^2}{d\xi^2}(\tfrac{d\xi}{d\eta})^2 + \tfrac{d}{d\xi} \cdot \tfrac{d^2\xi}{d\eta^2} \ , \tag{3.41}$$

After applying the above chain rule on Eq. (3.30), we obtian

$$\xi \frac{d^2\theta}{d\xi^2} + (1-\gamma-\xi)\frac{d\theta}{d\xi} + \theta = 0 \ , \tag{3.42}$$

and the reduced boundary conditions are

$$\theta(\frac{Pr}{Lm^2}) = 1 \ \ , \quad \theta(0) = 0 \ . \tag{3.43}$$

Eq. (3.42) is similar to Kummer's D.E that's give Kummer confluent hypergeometric function $|\bar{F}|$,

$$\theta(\xi) = \frac{\xi^{\gamma}|\bar{F}|(-1+\gamma;1+\gamma;-\xi)}{(\frac{Pr}{Lm^2})^{\gamma}|\bar{F}(-1+\gamma;1+\gamma;-\frac{Pr}{Lm^2})} \ , \tag{3.44}$$

where $\gamma = \frac{Pr}{Lm^2}(mf_w + 1)$, the solution of Eq. (3.44) in terms of η it gives

$$\theta(\eta) = (e^{-m\eta})^{\gamma}\frac{|\bar{F}|(-1+\gamma;1+\gamma;-\frac{Pr}{Lm^2}e^{-m\eta})}{|\bar{F}|(-1+\gamma;1+\gamma;-\frac{Pr}{Lm^2})} \ , \tag{3.45}$$

and temperature gradient

$$\theta'(0) = (-m\gamma) + \left((\frac{Pr(\gamma-1)}{Lm^2(\gamma+1)})\frac{|\bar{F}|(\gamma;2+\gamma;-\frac{Pr}{Lm^2}}{|\bar{F}|(-1+\gamma;1+\gamma;-\frac{Pr}{Lm^2}}\right) \ , \tag{3.46}$$

3.2 Results and discussion

The ordinary nonlinear differential equations are solved with the help of mathematical software Maple. In this segment, we have covered the effects of volume fraction of nanoparticles (ϕ), suction/injection (f_w) and magnetic parametric (M) on velocity and temperature profile. Water has been used as a base fluid with fixed Prandtl number as ($\mathrm{Pr} = 6.2$).

Fig. 2 depicts impact of magnetic field parameter (M) upon velocity of boundary layer of Cu-nanofluid. It is evident, due to increased magnetic field, velocity has been declined. It is because of the fact that the drag force also referred as Lorentz force, appears when magnetic fields are used to the fluid. This force tends to slow down the fluid velocity in the boundary layer. The impact of volume fraction of nanoparticles upon velocity of the Cu-nanofluid boundary layer is demonstrated in Fig. 3. The increasing in volume fraction (ϕ) results, as reduction in velocity. Fig. 4 shows the significance of the suction/injection factor through the velocity inside the Cu-nanofluid boundary layer. When suction/injection parameter (f_w) is increased, it is noticed that the velocity decreases.

Fig. 5 depicts impact of magnetic field parameter (M) upon temperature of boundary layer of Cu-nanofluid. This is evident, due to increased magnetic field, temperature will also be increased. The impact of volume fraction of nanoparticles (ϕ) upon temperature of the Cu-nanofluid boundary layer is demonstrated in Fig. 6. The increasing in volume fraction (ϕ) results, an increment in temperature. Fig. 7 shows the significance of the suction/injection factor through on temperature inside the Cu-nanofluid boundary layer. When the suction/injection parameter (f_w) is increased, it is noticed that temperature also decreased.

Fig. 8 illustrate variation of skin friction against suction/injection (f_w).

Enhancing the suction/injection factor causes an increment in skin friction and shear stress, although involvement of magnetic factor M beneath the boundary layer causes a gain in shear stress, seen in this investigation. Fig. 9 displays variation in local Nusselt number against suction/injection f_w with the variation of magnetic parameter M, increasing in the magnetic field decrease Nusselt number and rate of heat transfer that means the hardness and the strength of the surface will be poor in the presence of magnetic field.

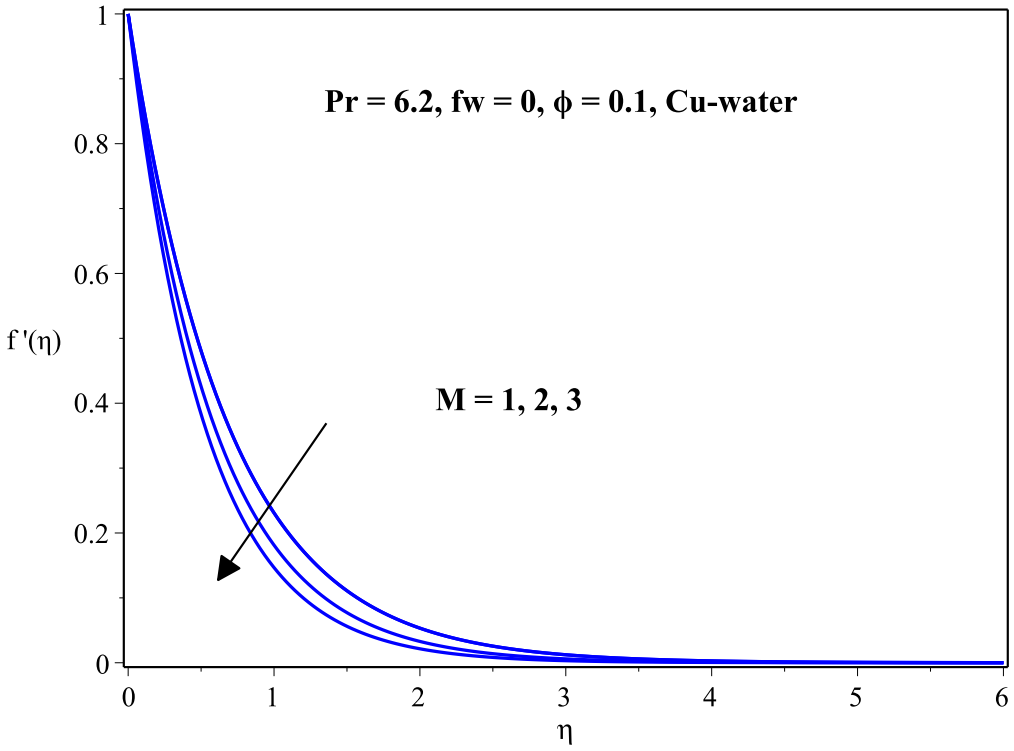

Fig. 2: Velocity profile for magnetic parameter M.

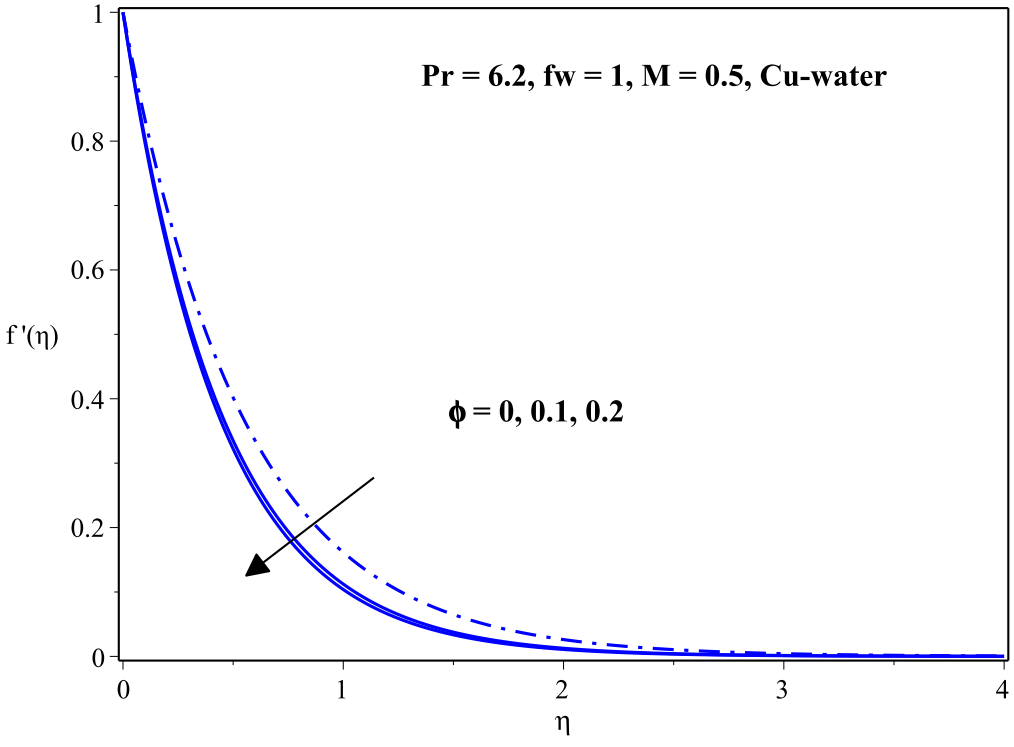

Fig. 3: Velocity profile for volume fraction ϕ.

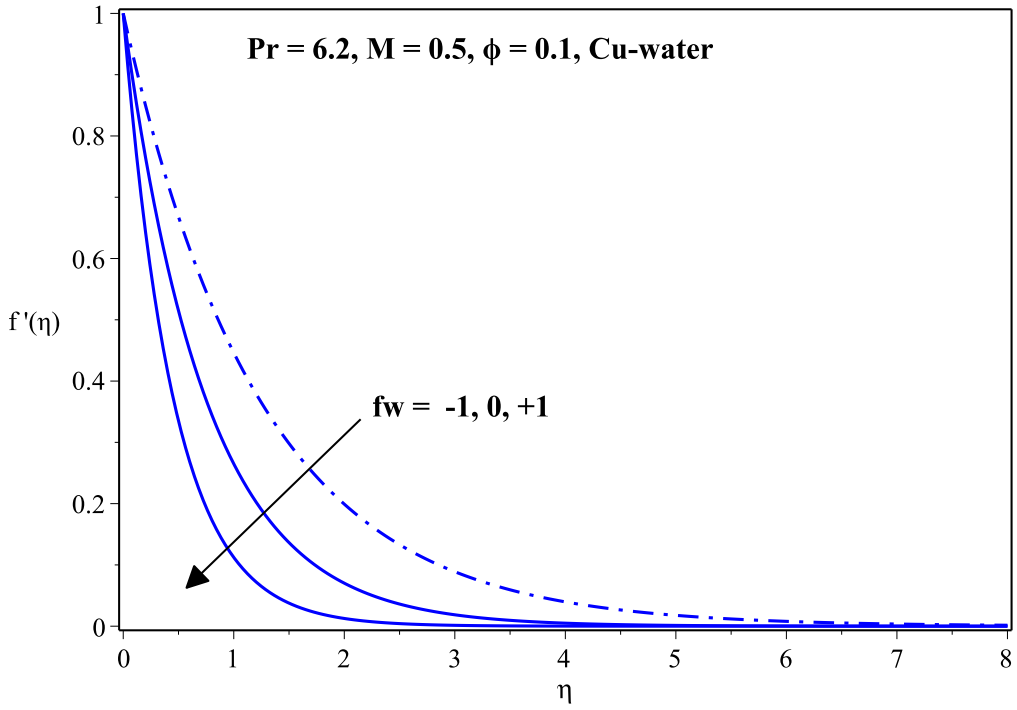

Fig. 4: Velocity profile for suction f_w.

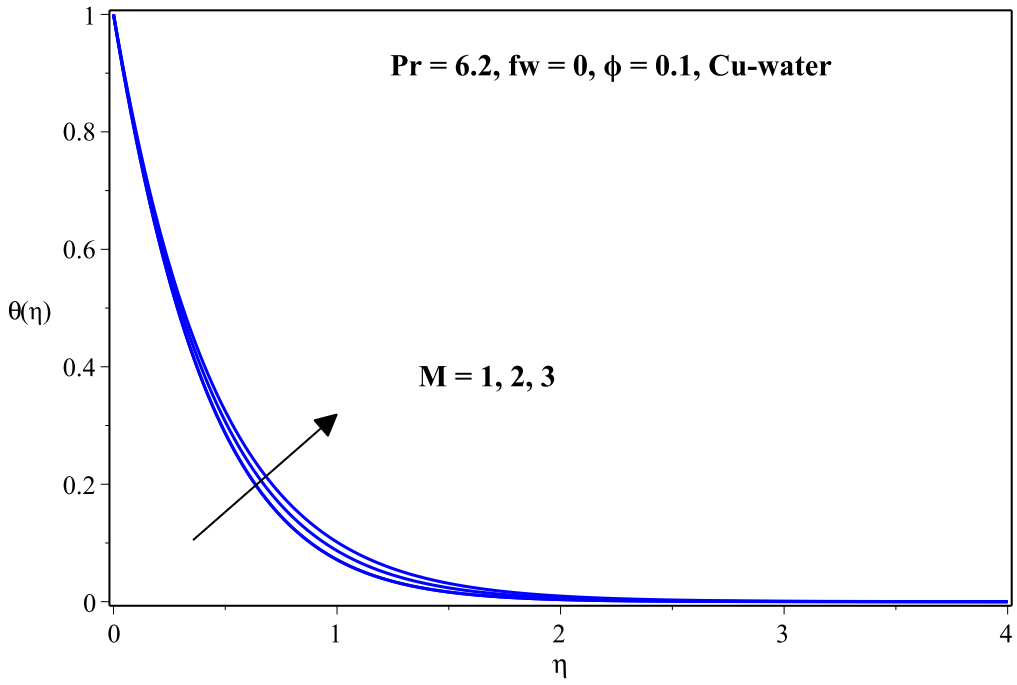

Fig. 5: Temperature profile for magnetic parameter M.

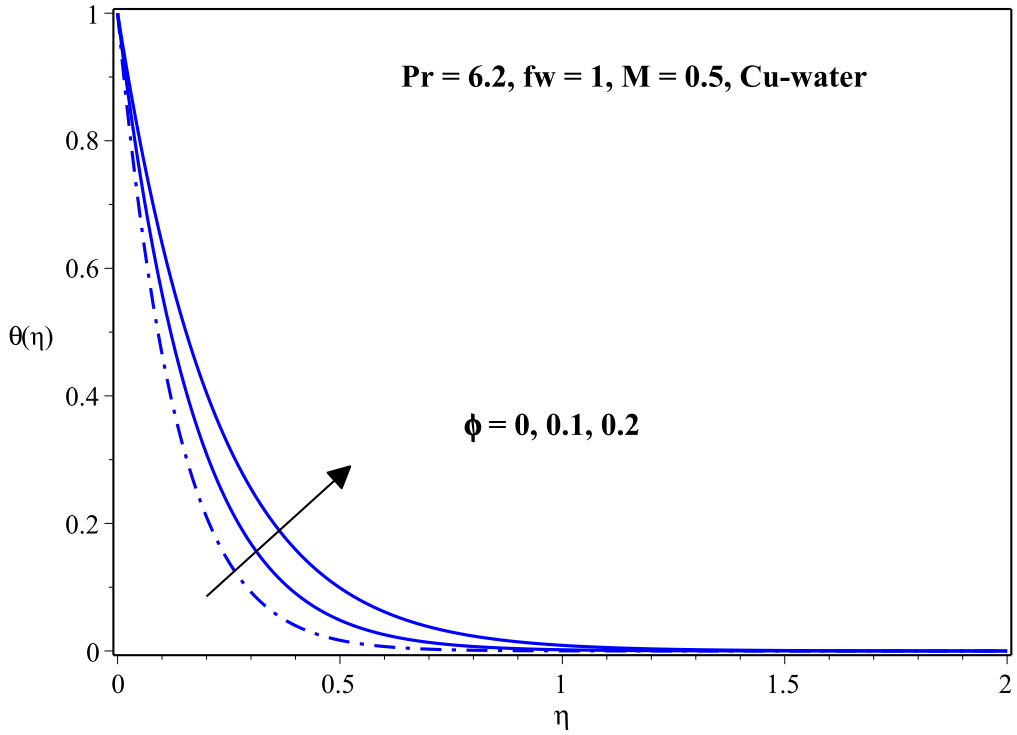

Fig. 6: Temperature profile for volume fraction ϕ.

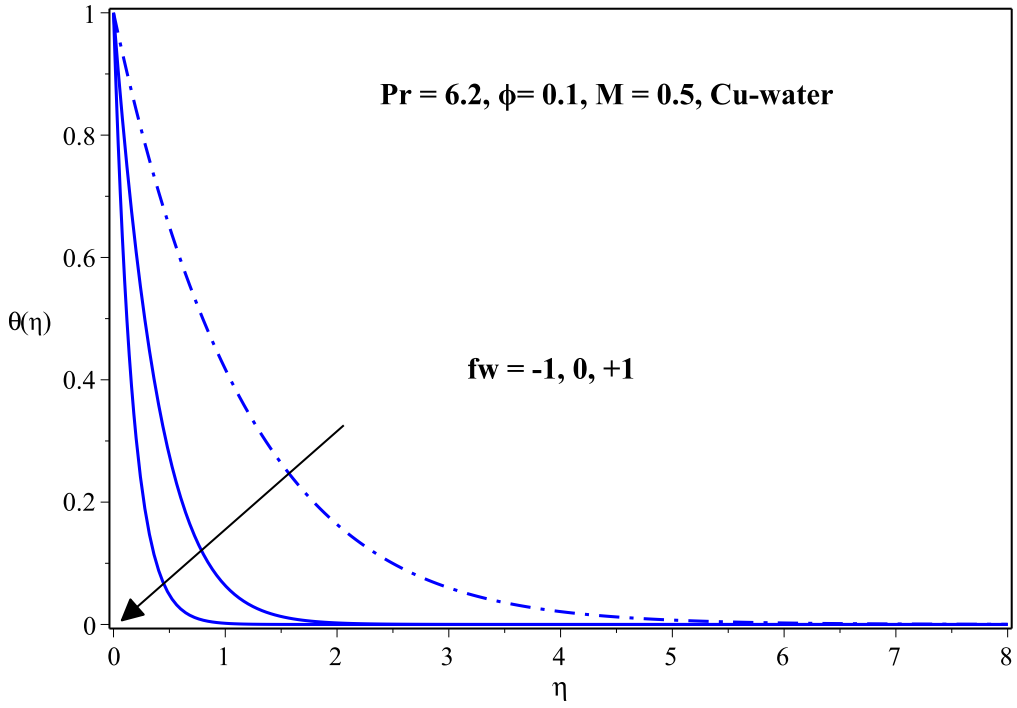

Fig. 7: Temperature profile for suction f_w.

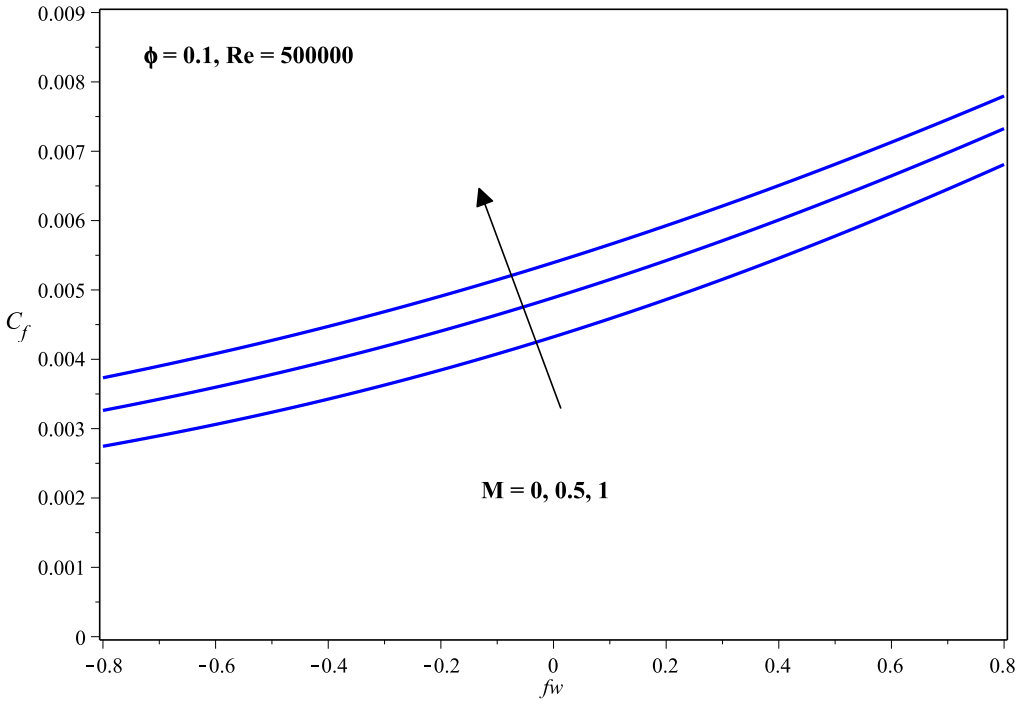

Fig. 8: Skin friction for suction/injection f_w.

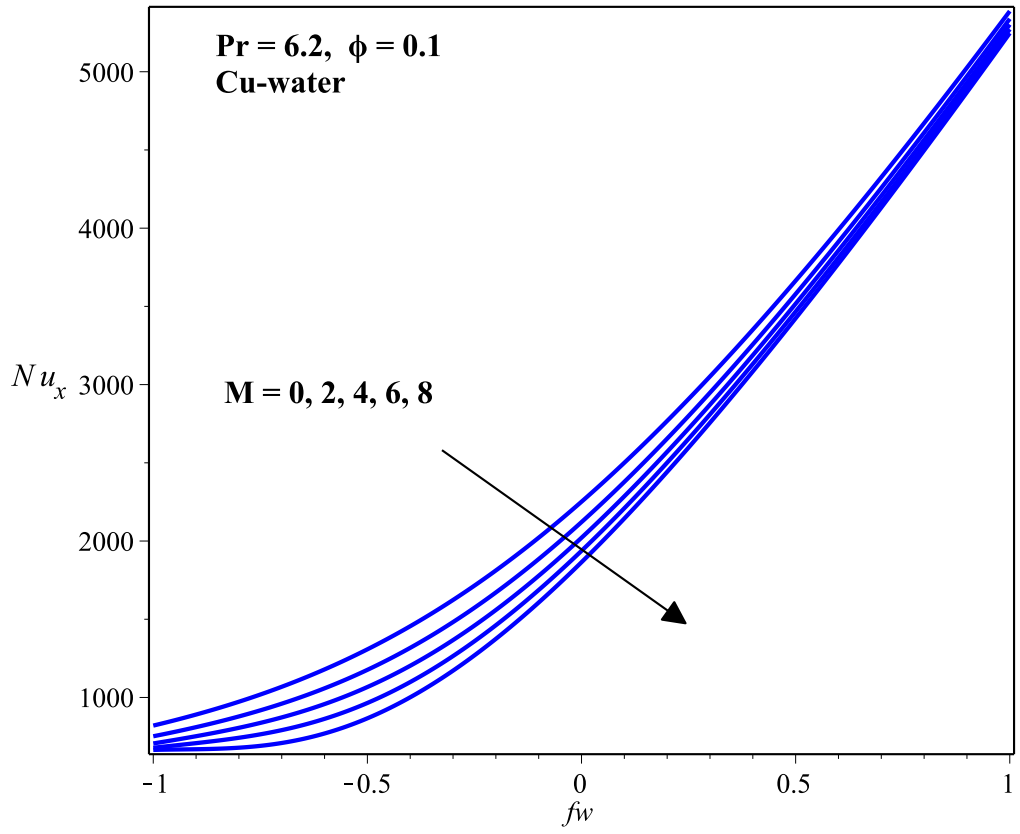

Fig. 9: Nusselt number for suction/injection f_w.

Chapter 4

Exact solution of nanofluid flow over a stretching / shrinking sheet with dual availability

This chapter is a continuation of the previous chapter by adding some new effects and constraints. The effect of a nanofluid particle (CuO) and viscous dissipation with thermal radiation is presented. There has been a comprehensive investigation of heat transfers of nanofluid by considering porous medium and viscous dissipation. Subsequently, mathematical formulation was modeled using boundary conditions. Using similarity variables, all PDEs of momentum and energy are converted into nonlinear ODEs for a formal formulation. At the end, nonlinear ODEs are solved by using Maple to get closed solution.

4.1 Mathematical modeling and exact solution

Consider 2-D, steady flow over a shrinking sheet in porous medium by considering the viscous dissipation effects. $\tilde{u}_w(x) = ax$ (where a is positive constant) is constant velocity of moving sheet. The governing equations are;

$$\frac{\partial \tilde{u}}{\partial x} + \frac{\partial \tilde{v}}{\partial y} = 0 \ , \tag{4.1}$$

$$\rho_{nf}(\tilde{u}\frac{\partial \tilde{u}}{\partial x} + \tilde{v}\frac{\partial \tilde{u}}{\partial y}) = \mu_{nf}\frac{\partial^2 \tilde{u}}{\partial y^2} - \sigma_{nf}\beta_0^2\tilde{u} - \mu_{nf}\frac{1}{K}\tilde{u} \ , \tag{4.2}$$

$$(\rho C_p)_{nf}(\tilde{u}\frac{\partial T}{\partial x} + \tilde{v}\frac{\partial T}{\partial y}) = k_{nf}\frac{\partial^2 T}{\partial y^2} + \mu_{nf}(\frac{\partial \tilde{u}}{\partial y})^2 + \sigma_{nf}\beta_0^2\tilde{u}^2 - \frac{\partial q_r}{\partial y}, \tag{4.3}$$

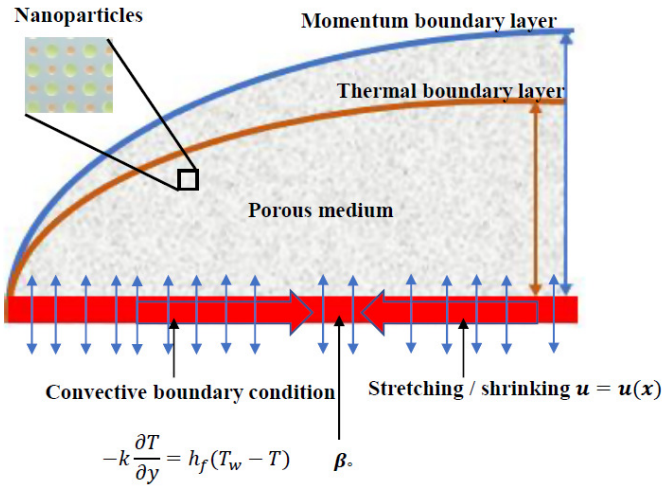

Fig. 10: Geometry of the problem.

Where velocity in x-direction is $\tilde{u}$, velocity in y-direction is $\tilde{v}$, T is the temperature,

Radiation heat flux q_r is possible to write by taking advantage of Rosseland approximation as

$$q_r = -(\frac{4\widehat{\sigma}}{3\widehat{K}})(\frac{\partial T^4}{\partial y}), \tag{4.4}$$

Here, $\widehat{K}$ is absorption co-efficient and $\widehat{\sigma}$ Stefan Boltzmann constant.

$T^4 \cong 4T_\infty^3 T - 3\bar{T}_\infty^4$,

By using T^4 in Eq.(4.4), we get

$$q_r = -(\frac{16\widehat{\sigma}\ T_\infty^3}{3\widehat{K}})(\frac{\partial T}{\partial y})\ , \tag{4.5}$$

so eq. (4.3) becomes

$$(\rho C_p)_{nf}(\tilde{u}\frac{\partial T}{\partial x}+v\frac{\partial T}{\partial y}) = k_{nf}\frac{\partial^2 T}{\partial y^2}+\mu_{nf}(\frac{\partial \tilde{u}}{\partial y})^2 + \sigma_{nf}\beta_0^2\tilde{u}^2+(\frac{16\widehat{\sigma}\ T_\infty^3}{3\widehat{K}})(\frac{\partial^2 T}{\partial y^2}), \qquad (4.6)$$

The boundary conditions for both the equations of momentum and energy are provided as;

$$\tilde{u}=\tilde{u}_w(x)=-ax,\ \ \tilde{v}=\tilde{v}_w \quad \text{at} \quad y=0\,, \qquad (4.7a)$$

$$\tilde{u}\ \rightarrow\ 0 \quad \text{as} \quad y\ \rightarrow\ \infty, \qquad (4.7b)$$

$$-k(\tfrac{\partial T}{\partial y})=\bar{h}_f(\tilde{T}_w-T) \quad \text{at} \quad y=0, \qquad (4.7c)$$

$$T\rightarrow\ T_\infty \quad \text{as}\ y\ \rightarrow\ \infty\,. \qquad (4.7d)$$

Where $T_w=T_\infty+bx$,

The physical properties of nanofluids are

$$\rho_{nf}=(1-\phi)\rho_f+\phi\rho_s\,, \qquad (4.8a)$$

$$(\rho C_p)_{nf}=(1-\phi)(\rho C_p)_f+\phi(\rho C_p)_s\,, \qquad (4.8b)$$

$$\frac{\sigma_{nf}}{\sigma_f}=1+\frac{3(\frac{\sigma_s}{\sigma_f}-1)\phi}{(\frac{\sigma_s}{\sigma_f}+2)-(\frac{\sigma_s}{\sigma_f}-1)\phi}\,, \qquad (4.8c)$$

Brownian movement has major effects on thermal conductivity. According to *Koo and Kleinstreuer* [27, 28] effective thermal conductivity made up of two parts: static portion and Brownian motion portion. The Brownian motion has significant consequence on thermal conductivity.

$$k_{nf}=k_{static}+k_{Brownian}, \qquad (4.9)$$

k_{static} is static thermal conductivity according to Maxwell.

$$\frac{k_{static}}{k_f} = 1 + \frac{3(\frac{k_p}{k_f} - 1)\phi}{(\frac{k_p}{k_f} + 2) - (\frac{k_p}{k_f} - 1)\phi} , \tag{4.10}$$

$$k_{Brownian} = 5 \times 10^4 (\rho C_p)_f \, \beta \, \phi \sqrt{\frac{k_b T^*}{d_p \rho_p}} \, g(T^*, \phi) , \tag{4.11}$$

Where, β and g are two empirical functions. Later Li [28] updated the KKL model by merging β and g into a new function G and introducing a thermal interfacial resistance $R_f = 4 \times 10^8 km2/W$ the initial k_p renewed by a new $k_{p.eff}$ in the genre of

$$R_f = \frac{d_p}{k_p} = \frac{d_p}{k_{p.eff}} , \tag{4.12}$$

The function G will have a varied function depending on the kind of nanoparticles and based fluid. Only water is utilized as a base fluid in this application. This function has the following format for CuO-water nanofluids.

$$\begin{aligned} G(T^*, \phi, d_p) =& (b_1 + b_2 \; ln(d_p) + b_3 \; ln(\phi) + b_4 ln(\phi) \; ln(d_p) + b_5 \\ & ln(d_p)^2) \; ln(T^*) + (b_6 + b_7 \; ln(d_p) + a_8 \; ln(\phi) + b_9 \\ & ln(d_p) \; ln(\phi) + b_{10} \; ln(d_p)^2) \; , \end{aligned} \tag{4.13}$$

In Table 3, above co-efficients are given, Finally KKL correlation can be written as

$$k_{Brownian} = 5\times10^4\,\phi\,(\rho C_p)_f\sqrt{\frac{k_b T^*}{\rho_p d_p}}\,G(T^*,\phi,d_P)\,, \tag{4.14}$$

μ_{nf} can be written as viscosity

$$\mu_{nf} = \mu_{static}+\mu_{Brownian} = \mu_{static}+\frac{k_{Brownian}}{k_f}\times\frac{\mu_f}{Pr_f}, \tag{4.15}$$

where $\mu_{static} = \frac{\mu_f}{(1-\phi)^{2.5}}$

Table 2: Thermal properties of CuO and water [27, 28]

Physical properties	**Base fluid (water)**	**Nanoparticle** (CuO)
C_p(J/kgK)	4179	540
ρ(kg/m^3)	997.1	6500
k(W/mK)	0.613	18
d_p	-	29
σ $(\Gamma.m)^{-1}$	0.05	10^{-10}

To convert the governing PDEs into dimensionless ODEs, have used the similarity transformation,

$$\tilde{u} = axf'(\eta),\quad \tilde{v} = -(a\nu)^{1/2}f(\eta),\quad \eta = y\sqrt{\frac{a}{\nu}},\quad \theta(\eta) = \frac{T-\bar{T}_\infty}{\bar{T}_w-\bar{T}_\infty}, \tag{4.16}$$

Table 3: Thermal properties of CuO and water [27, 28]

Coefficient vlues	**CuO-water**
b_1	-26.593310846
b_2	-0.403818333
b_3	-33.3516805
b_4	-1.915825591
b_5	$6.42185846658e^{-2}$
b_6	48.40336955
b_7	-9.787756683
b_8	190.245610009
b_9	10.9285386565
b_{10}	-0.72009983664

Applying above Eqs. (4.16) and (4.8(a, b, c)) in Eqs. (4.2), (4.2) and (4.6), we get

$$A_2 f'''+A_1(ff''-f'^2)-(MA_6+\Phi\, A_2)\, f' = 0\,, \tag{4.17}$$

$$(A_4 + Rd)\, \theta'' + A_3 Pr(f\theta' - f'\theta) + Pr \;\; A_2 Ecf''^2$$

$$+ \;\; A_6 PrMEcf'^2 = 0 \tag{4.18}$$

$$f(0) = f_w,\; f'(0) = -\tfrac{c}{a} = -\lambda,\; f'(\infty) = 0\,, \tag{4.19}$$

$$\theta'(0) = -Bi[1 - \theta(0)],$$

$$\theta(\eta) \to 0, \ when \ \eta \ \to \ \infty \, , \tag{4.20}$$

The physical parameters are specified as follows:

$$Pr = \frac{\nu_f(\rho C_p)_f}{k_f}, \quad M = \frac{\sigma_f \beta_0^2}{a\rho_f}, \quad \Phi = \frac{\mu_f}{\rho_f a K}, \quad Bi = \frac{h_f}{k}\sqrt{\frac{\nu_f}{a}},$$

$$Ec = \frac{(ax)^2\rho_f}{(\rho Cp)_f(\bar{T_w} - \bar{T_\infty})}, \quad Rd = \frac{16\widehat{\sigma}T_\infty^3}{3\widehat{K}k_f}, \quad f_w = \frac{v_w}{\sqrt{a\nu_f}},$$

$$A_1 = \frac{\rho_{nf}}{\rho_f}, \quad A_2 = \frac{\mu_{nf}}{\mu_f}, \quad A_3 = \frac{(\rho Cp)_{nf}}{(\rho Cp)_f}, \quad A_4 = \frac{k_{nf}}{k_f}, \quad A_5 = \frac{\sigma_{nf}}{\sigma_f}, \tag{4.21}$$

C_f and Nu_x are expressed below;

$$C_f = 2\frac{\tau_w}{U_w^2} = \frac{-2m}{\sqrt{Re}(1-\phi)^{2.5}} \ , \tag{4.22}$$

where, $Re_x = (ax^2/\nu)$, local Reynolds number,

$$Nu_x = \frac{xq_W}{k_f(T_w - T_\infty)} = -(A_4 + Rd)\sqrt{Re}\ \theta'(0), \tag{4.23}$$

where

$$q_w = -\left(k_{nf} + (\tfrac{16\widehat{\sigma}\ T_\infty^3}{3\widehat{K}})\right)(\tfrac{\partial T}{\partial y})_{y=0}.$$

4.2 Methodology

By assuming the solution, we get exact solution of Eq. (4.17) satisfying boundary conditions.

$$f(\eta) = f_w - \frac{\lambda}{m}(1 - e^{-m\eta}), \tag{4.24}$$

Using the above equation in Eq. (4.17), we get

$$B_1 m^2 - f_w m + \lambda - B_1 B_2 M - B_1 \Phi = 0, \tag{4.25}$$

where $B_1 = A_2/A_1, \quad B_2 = A_5/A_2,$
so the solution of (4.25) is

$$m = \frac{f_w \pm \sqrt{{f_w}^2 + 4B_1(B_1 B_2 M + B_1 \Phi - \lambda)}}{2B_1}, \tag{4.26}$$

Hence dual solution (4.26) of the proposed problem is accessible.

$$f'(\eta) = -m\lambda e^{-m\eta},$$

so velocity components become

$$\tilde{u} = -ax\lambda e^{-m\eta}, \quad and \quad \tilde{v} = -\sqrt{a\nu}(f_w - \frac{\lambda}{m}(1 - e^{-m\eta})), \tag{4.27}$$

To find the solution of eq.(4.18), we establish a new variable ξ,

$$\xi = e^{-m\eta}, \tag{4.28}$$

By turning Eqs. (4.24) and (4.28) into account Eqs. (4.18) and (4.20), we get

$$\xi\frac{d^2\theta}{d\xi^2}+(1+\gamma+h\xi)\frac{d\theta}{d\xi}+h\theta+\frac{PrEc\lambda^2}{C}(A_2+\frac{MA_5}{m^2})\xi = 0, \tag{4.29}$$

The boundary conditions will be formulated as having:

$$\theta(0) = 0, \quad \theta'(1) = \frac{Bi}{m}[1-\theta(1)], \tag{4.30}$$

where $h = \frac{PrA_3\lambda}{m^2C}, \quad \gamma = -h(\frac{f_w m}{\lambda} - 1), \quad C = A_4 + Rd,$

By solving Eq. (4.29), we obtain

$$\begin{aligned}\theta(\xi) =& e^{-h\xi}hyp.(\gamma,[1+\gamma],h\xi)C_2 + e^{(}h\xi)\xi^{\gamma}C_1 \\ & -\frac{1}{2}\,\frac{PrEc\lambda^2(A_2m^2+A_5M)(h\xi-\gamma-1)}{h^2m^2C},\end{aligned} \tag{4.31}$$

By applying boundary conditions and putting the value of ξ in (4.31), the final solution is,

$$\theta(\eta) = -\frac{1}{2h^2m^2C}(e^{he^{-m\eta}}hyp.([\gamma],[1+\gamma],he^{-m\eta})EcPr\lambda^2(A_2m^2\gamma + A_2m^2 + A_5M\gamma + A_5M)) + \frac{1}{2((-hm - m\gamma + Bi)h^2e^{-h}m^2C)}((e^{-}hEcPr\lambda^2A_5Mhyp.([1+\gamma],[2+\gamma],h)\gamma hm + e^{-h}hyp.([\gamma],[1+\gamma],h)EcPr\lambda^2BiA_5M\gamma - e^{-h}EcPr\lambda^2A_2hyp.([\gamma],[1+\gamma],h)m^3\gamma h + e^{-h}hyp.([\gamma],[1+\gamma],h)EcPr\lambda^2BiA_2m^2\gamma - EcPr\lambda^2BiA_5M\gamma - e^{-h}EcPr\lambda^2A_5Mhyp.([\gamma],[1+\gamma],h)m\gamma h - EcPr\lambda^2BiA_2m^2\gamma + e^{-h}EcPr\lambda^2A_2hyp.([1+\gamma],[2+\gamma],h)m^3\gamma h - e^{-h}EcPr\lambda^2A_2hyp.([\gamma],[1+\gamma],h)m^3h + e^{-h}hyp.([\gamma],[1+\gamma],h)EcPr\lambda^2BiA_5M + EcPr\lambda^2BiA_2hm^2 - EcPr\lambda^2BiA_2m^2 - e^{-h}EcPr\lambda^2A_5Mhyp.([\gamma],[1+\gamma],h)hm + EcPr\lambda^2A_2m^3h + 2Bih^2m^2C - EcPr\lambda^2BiA_5M + e^{-h}hyp.([\gamma],[1+\gamma],h)EcPr\lambda^2BiA_2m^2 - EcPr\lambda^2A_5Mhm + EcPr\lambda^2BiA_5Mh)e^{he^{-m\eta}}(e^{-m\eta})^{-\gamma}) - \frac{PrEc\lambda^2(A_2m^2 + A_5M)(he^{-m\eta}) - \gamma - 1}{2h^2m^2C}. \tag{4.32}$$

4.3 Results and discussion

In this erudition, put on view to moving continuous surface enclosed by nanofluid under the involvement of magnetic field and thermal radiations. The partial differential equations (PDEs) transformed into ordinary differential equations which are solved analytically. In order to generate exact solutions for the specified problem of boundary value an algorithm built by the Maple software. Consequences for temperature profile, skin friction co-efficient, velocity profile and local Nusselt number displayed against a variety of influencing factors, porosity (Φ), magnetic parameter (M), shrinking parameter (λ), suction injection (f_w), Eckert number (Ec) with an inflexible value of Prandtl ($Pr = 6.2$) and volume fraction ($\phi = 0.04$). The upper branch associated with solution of positive ($+$) part of the eq. (4.26) and lower branch associated with solution of negative ($-$) part of eq. (4.26).

Figs. (11 - 14) illustrate the fluctuation of f_w, Φ, M, and λ on the solution area for m, with changes occurring among each region of the solution. Changing the values of the parameters (f_w, Φ, M and λ) may have an impact on the solution m in the appropriate way. Fluctuation in skin friction as a function of several factors are presented in Figs. (15 - 18). Figs. 15 evidently indicates that rising λ leads to an increases in skin friction co-efficient C_f for suction when $f_w > 0$, it decreases for injection when $f_w < 0$. It can be seen in Fig. 16 that skin friction C_f rises with increasing porosity (Φ) for suction when $f_w > 0$ and it decreases for injection when $f_w < 0$. It is discovered in Fig. 17 that when values of Φ rise, C_f diminishes in both the lower and upper regions. It is determined in Fig. 17 that raising suction parameter f_w increases skin friction co-efficient for $\lambda > 0$ and decreases for $\lambda < 0$.

Figs. (19 - 22) are illustrated to assess the dimensionless velocity profile for different effects of f_w, λ, M, and Φ correspond to lower and upper

branches. This can also be indicated in Fig. 19 that velocity reduces with increasing f_w in lower solution, while velocity rises with growing f_w in upper branch. Since suction f_w is directly proportional to skin friction co-efficient, so due to increment in skin friction, momentum boundary layer has been compressed. When λ burgeoning, velocity is varying directly in lower solution but in upper solution velocity varies inversely as delineated in Fig. 20. The response of magnetic parameter M is seen in Fig. 21, fluid velocity is observed to decrease as M rises for lower branch. It is because of the fact that the drag force also referred as Lorentz force, appears when magnetic fields are used to the fluid. This force tends to slow down the fluid velocity in the boundary layer but The upper branch is mounting as magnetic parameter M rises. The consequences of porosity (Φ) is appeared in Fig. 22, velocity decline with increasing porous parameter Φ in lower branch, at the same moment it varies directly in upper branch.

The impact of various parameters such as suction f_w, stretching λ, radiation Rd, Eckert number Ec, and Biot number Bi on lower and upper branches of temperature profile are indicated in Figs. (23 - 27). The temperature decreases with increasing f_w in both branches (upper and lower) can be seen in Fig. 23. It delineated in fig. 24 that temperature is varying inversely to λ either in lower and upper branches. The consequences of radiation factor (Rd) appears in fig. 25 temperature declined with rising of Rd in both branches. It demonstrates in fig. 26 that raising Eckert number Ec leads into an increase in temperature on both solutions. In Fig. 27, It is noticed that the temperature profile improves as the biot number rises on lower and upper branches. So the temperature relies on the convective heat transfer coefficient, heat transfer is directly proportional to heat transfer coefficient.

Fig. 28 displays variation in local Nusselt number against suction/injection

f_w with the variation of magnetic parameter M, increasing in the magnetic field decrease Nusselt number and rate of heat transfer in upper branch, that means the hardness and the strength of the surface will be poor in the presence of magnetic field and opposite behavior seen in the lower branch.

At the end, Fig. 29 - 32 stream function ψ is plotted and compared for the cases of suction/injection with fixed values $M = 0.2, \Phi = 0.2$ and $\lambda = 1.5$ for both lower and upper branches.

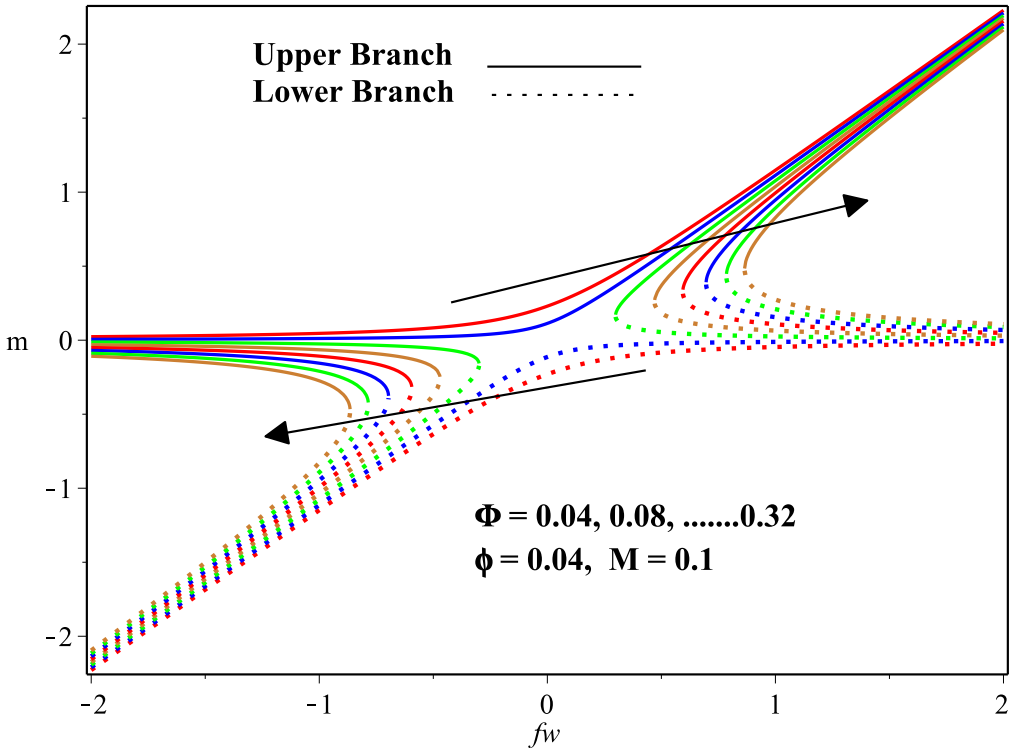

Fig. 11: Relation of m vs suction f_w.

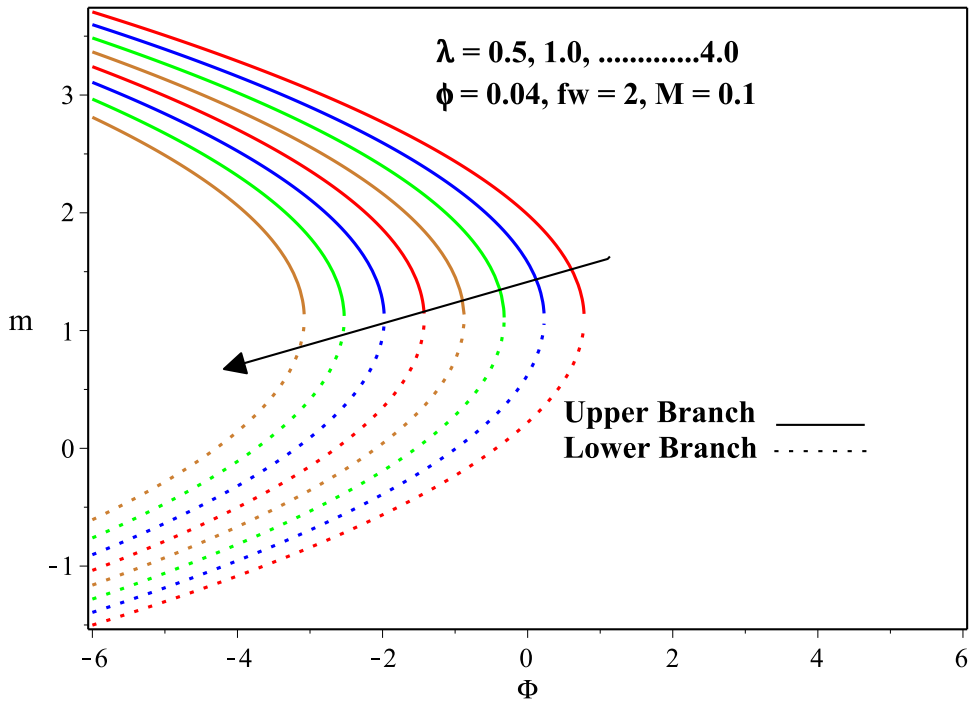

Fig. 12: Relation of m vs porosity Φ.

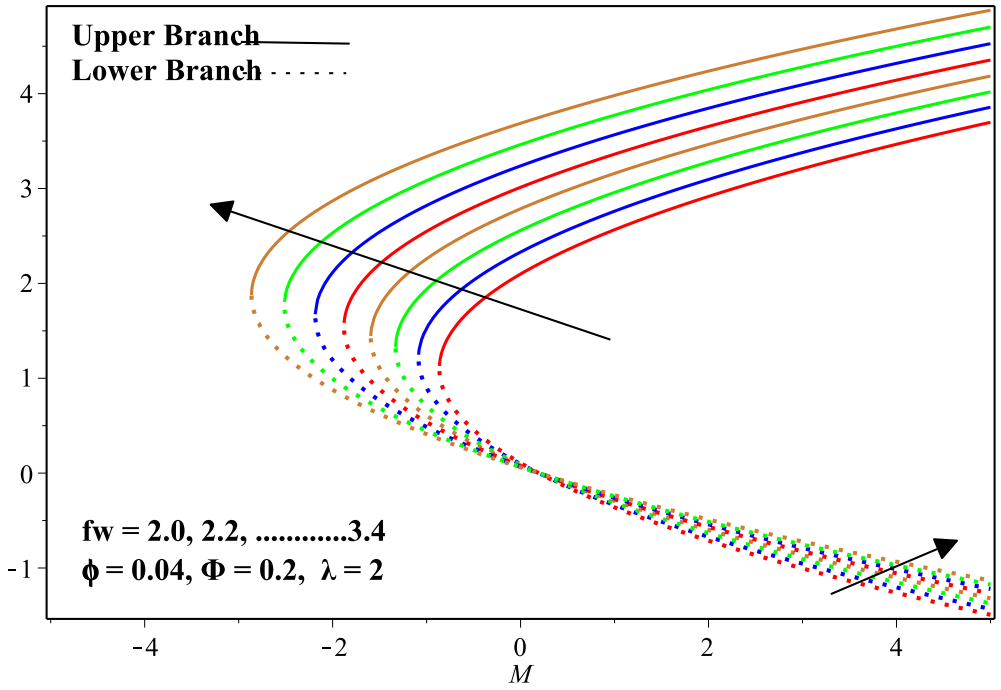

Fig. 13: Relation of m vs magnetic parameter M.

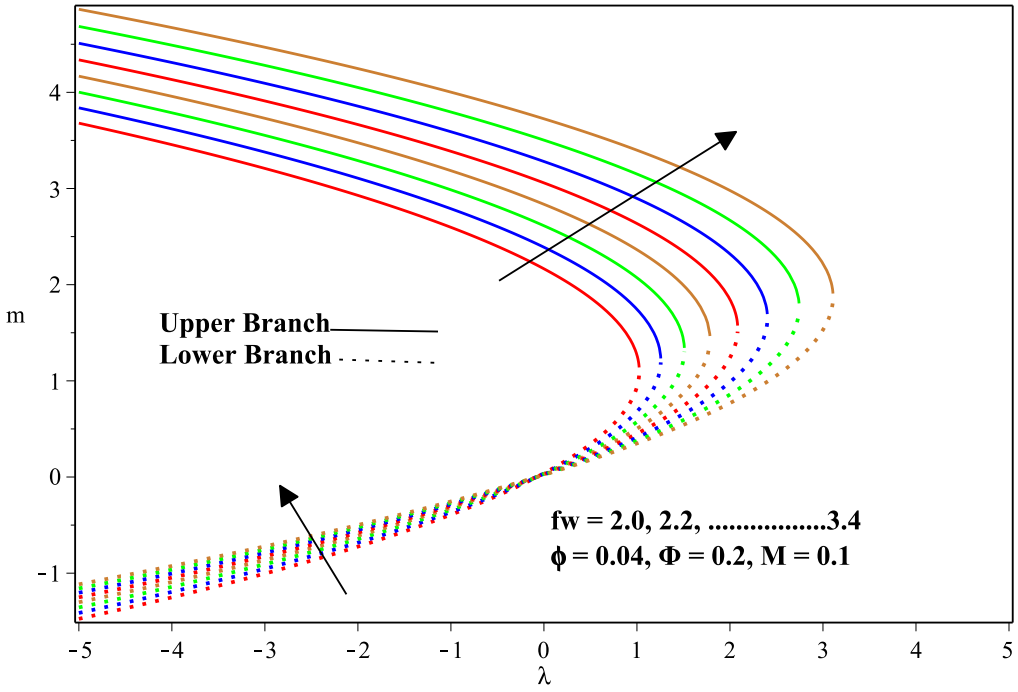

Fig. 14: Relation of m vs stretching parameter λ.

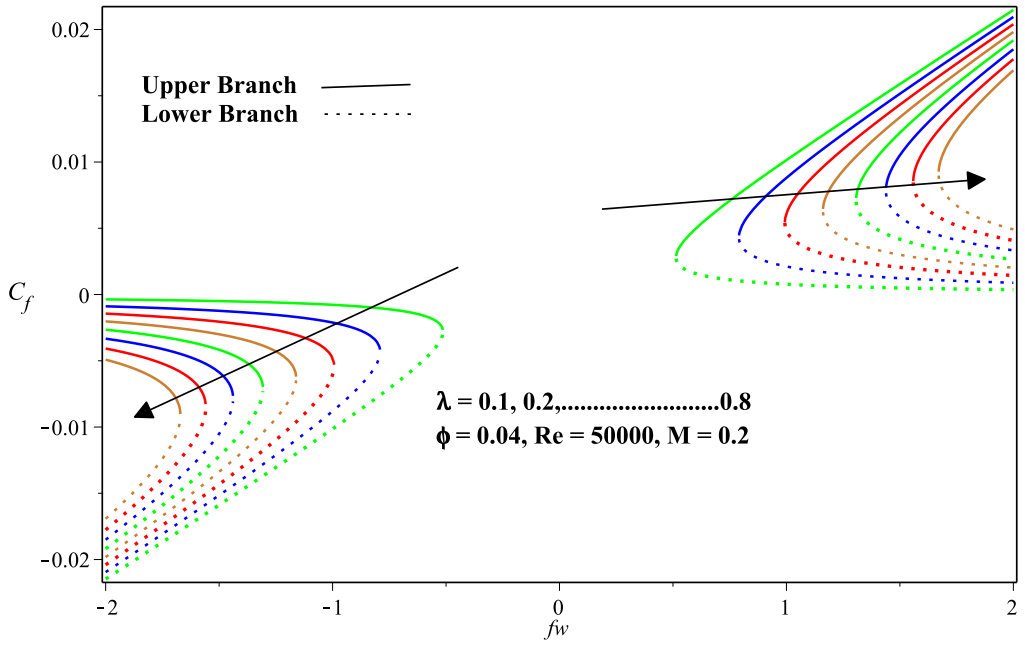

Fig. 15: Fluctuations of skin friction for stretching parameter λ.

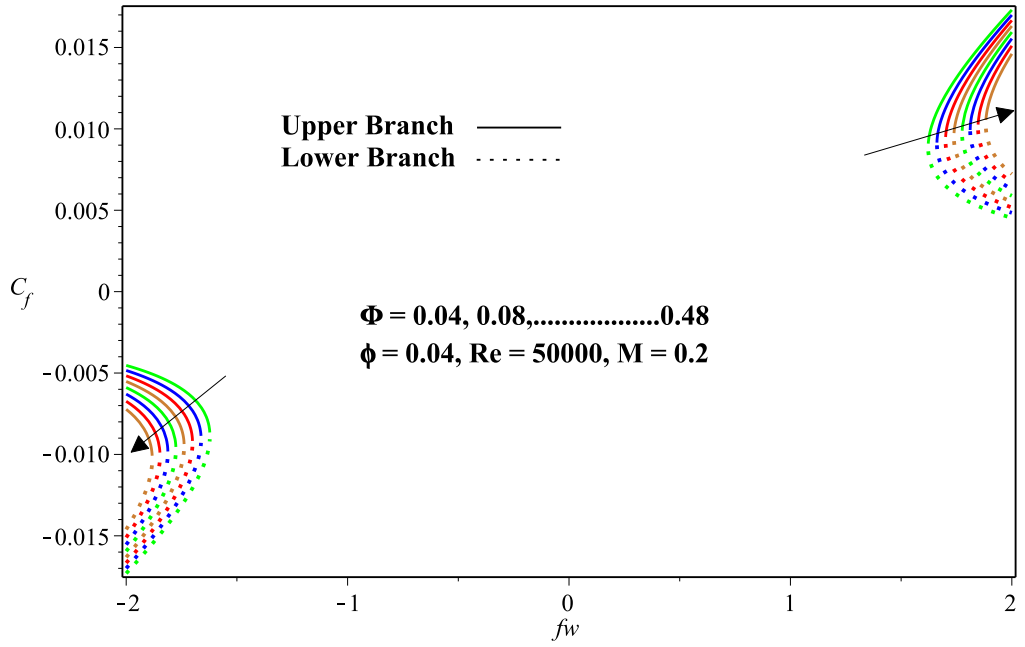

Fig. 16: Fluctuations of skin friction for porosity Φ.

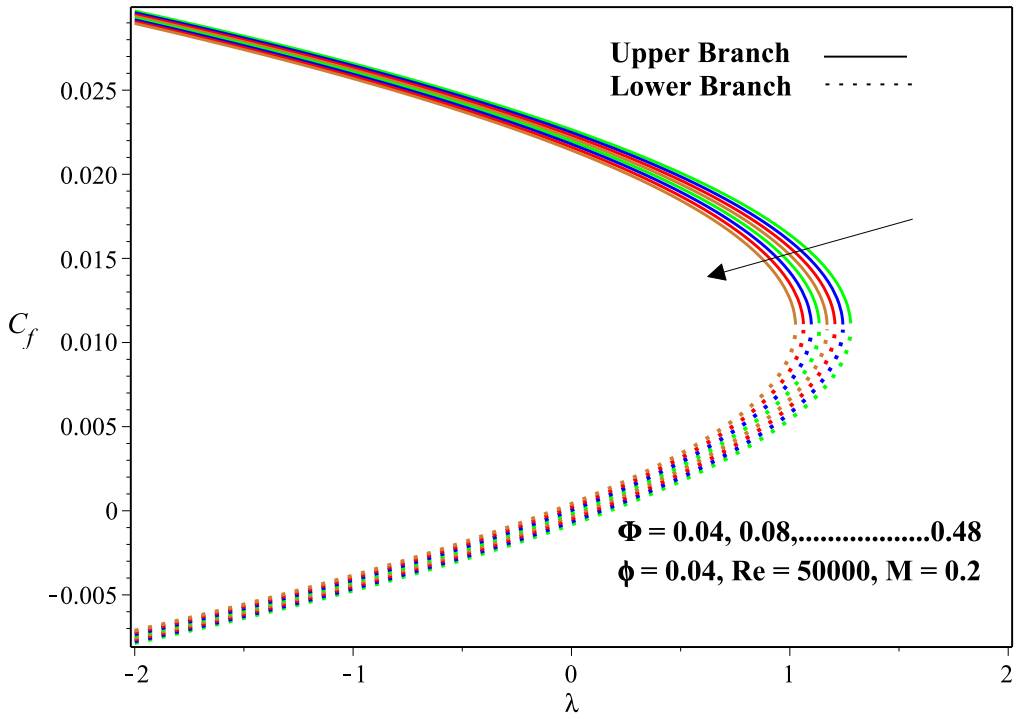

Fig. 17: Skin friction as shrinking/stretching for porosity Φ.

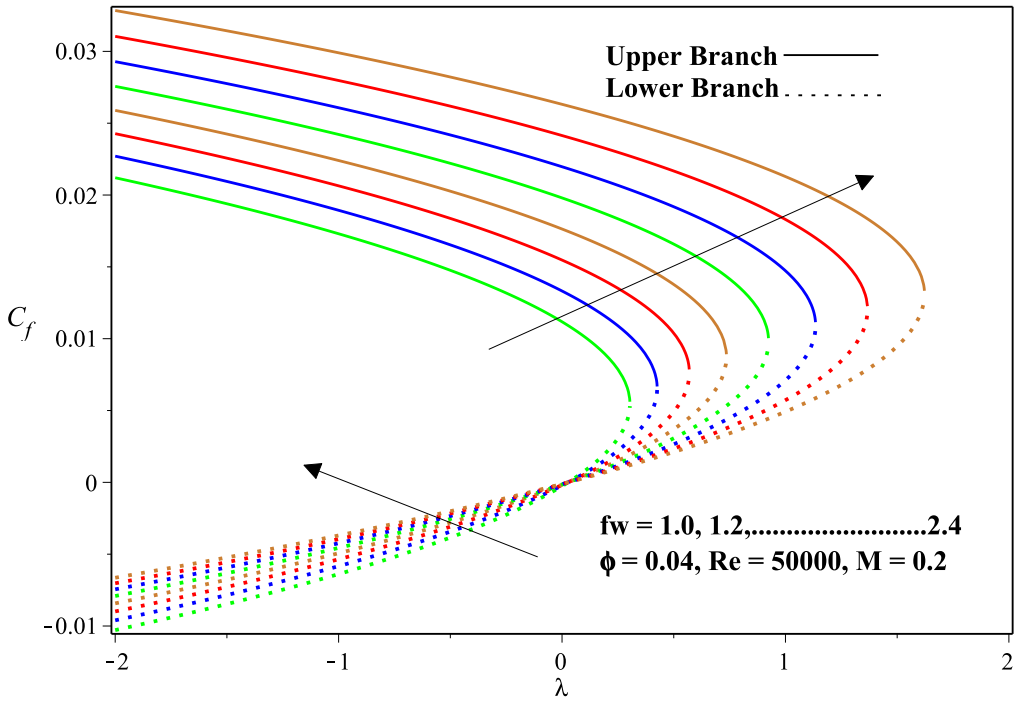

Fig. 18: Fluctuations of skin friction for suction f_w.

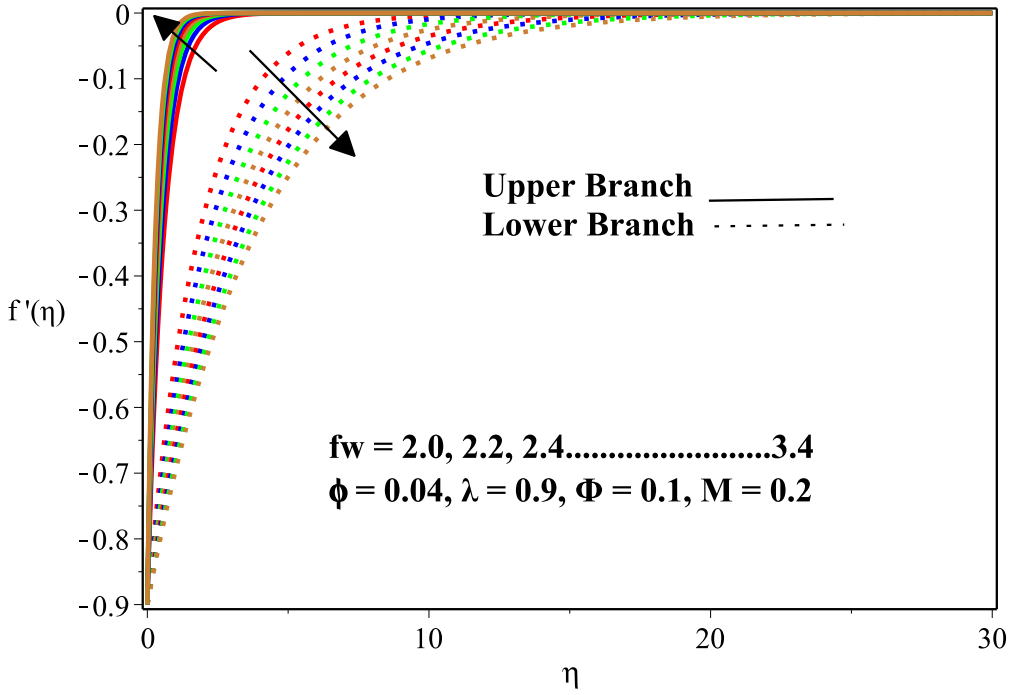

Fig. 19: Velocity profile for suction parameter f_w.

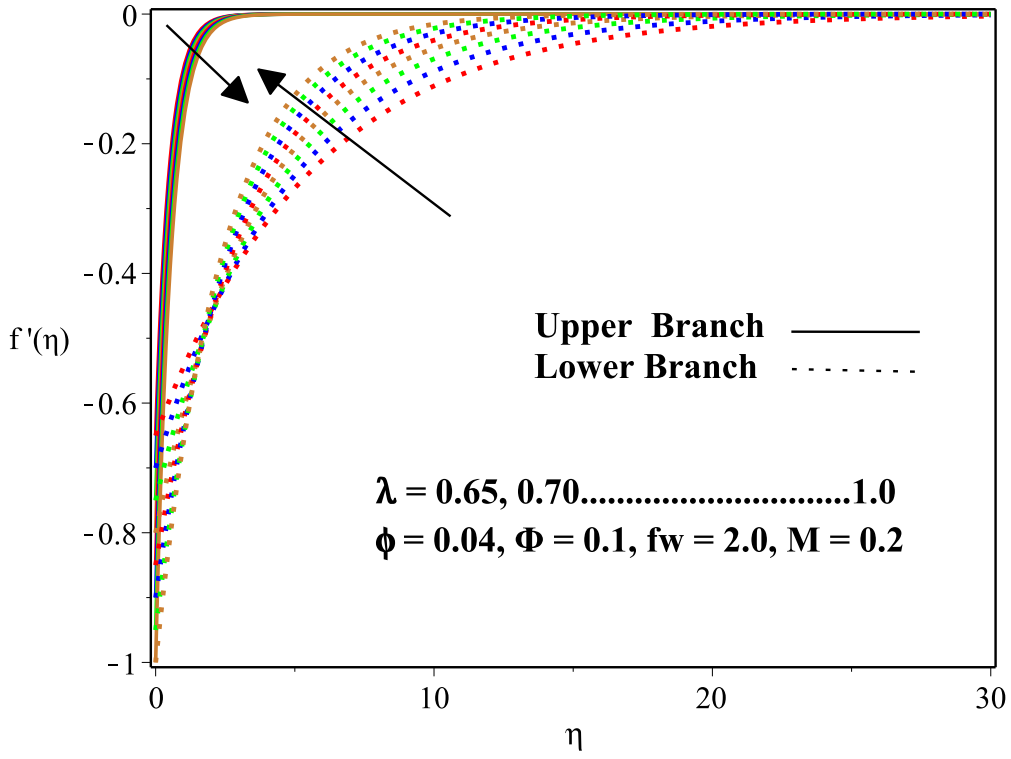

Fig. 20: Velocity profile for stretching parameter λ.

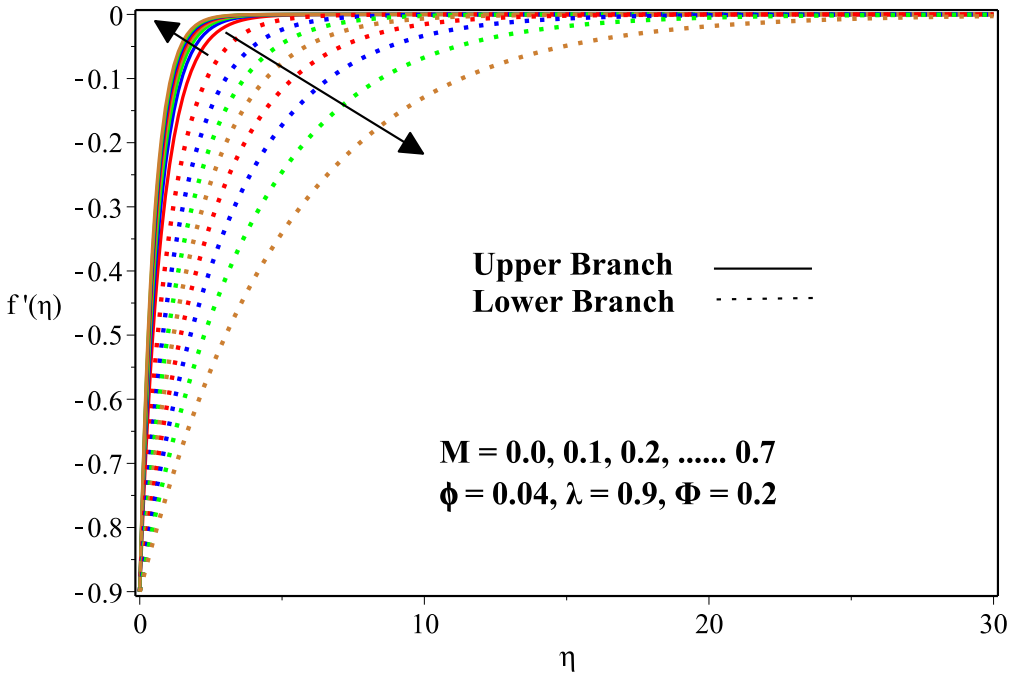

Fig. 21: Velocity profile for magnetic parameter M.

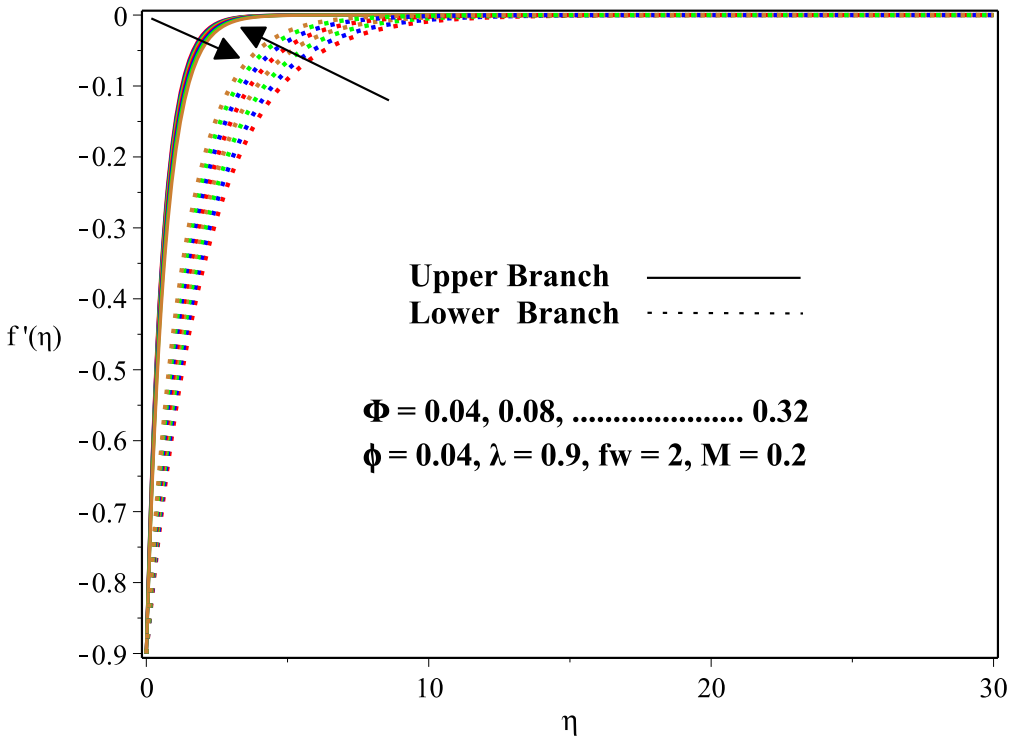

Fig. 22: Velocity profile for porosity Φ.

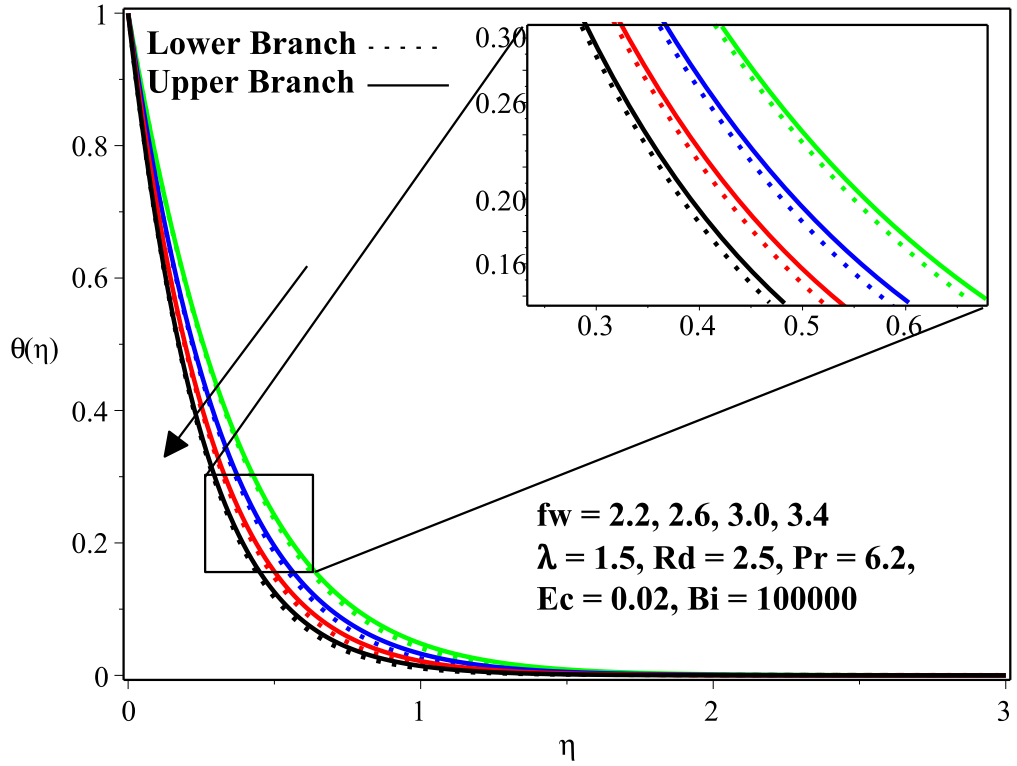

Fig. 23: Temperature profile for suction parameter f_w.

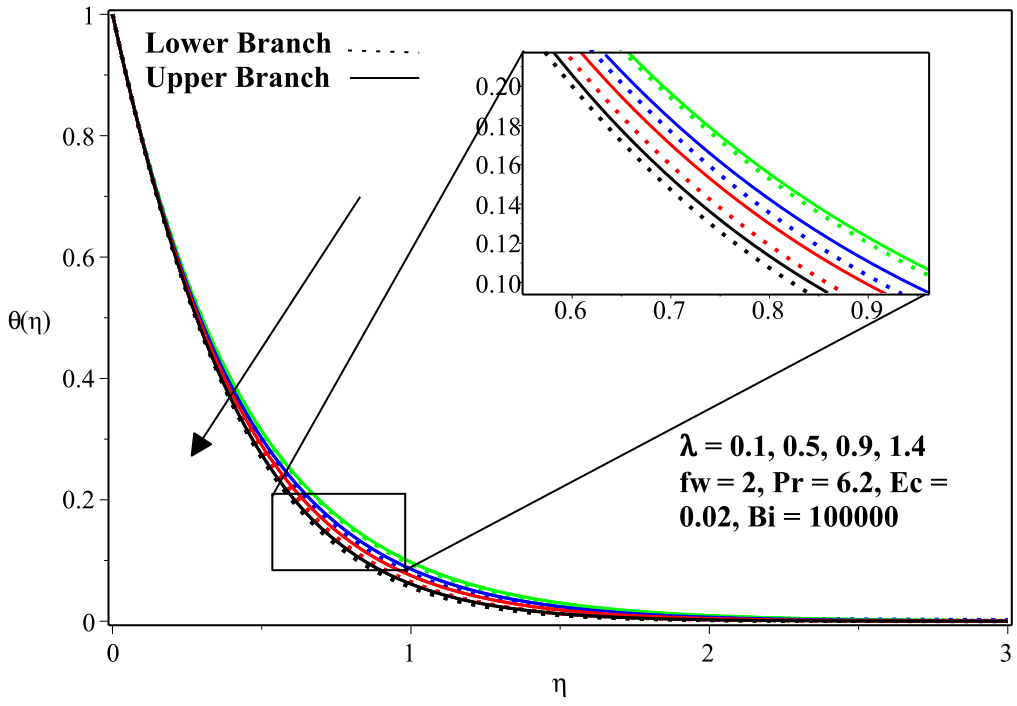

Fig. 24: Temperature profile for stretching λ.

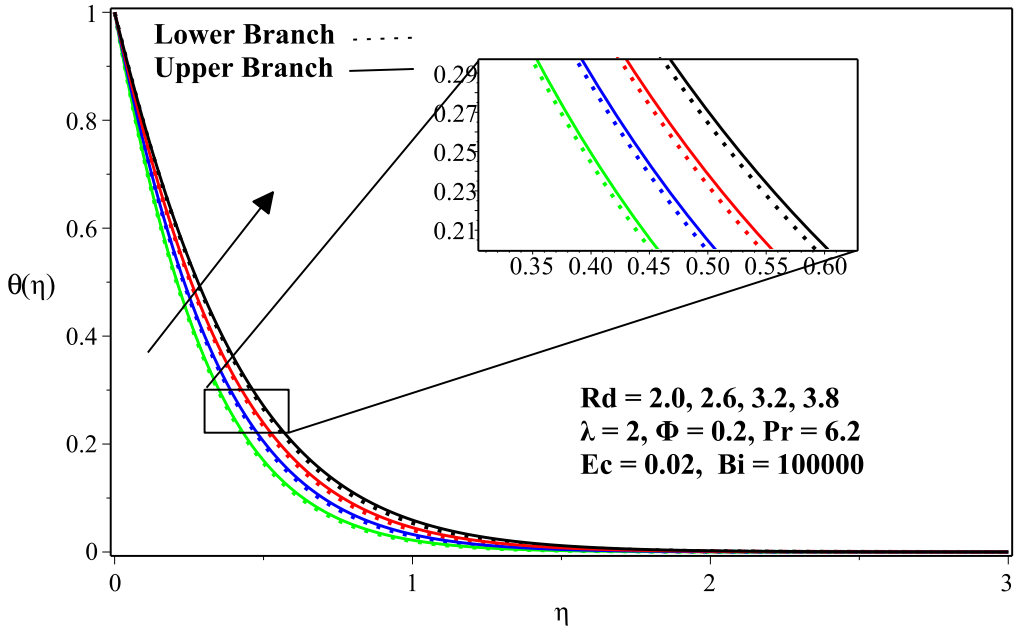

Fig. 25: Temperature profile for radiation parameter *Rd*.

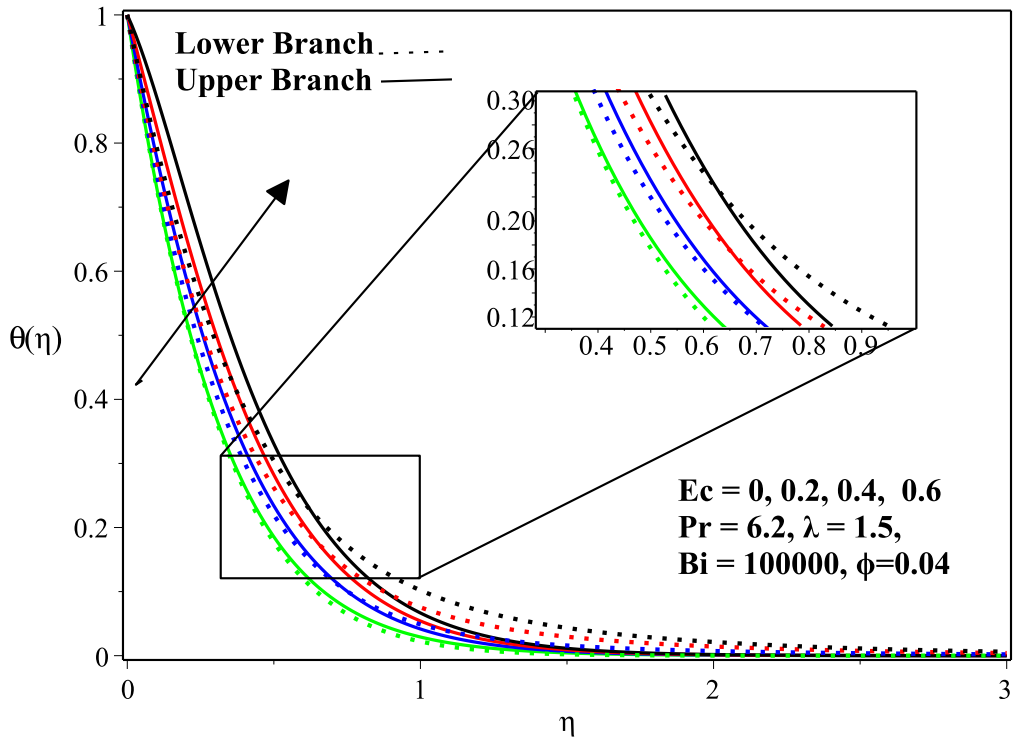

Fig. 26: Temperature profile for Eckert number *Ec*.

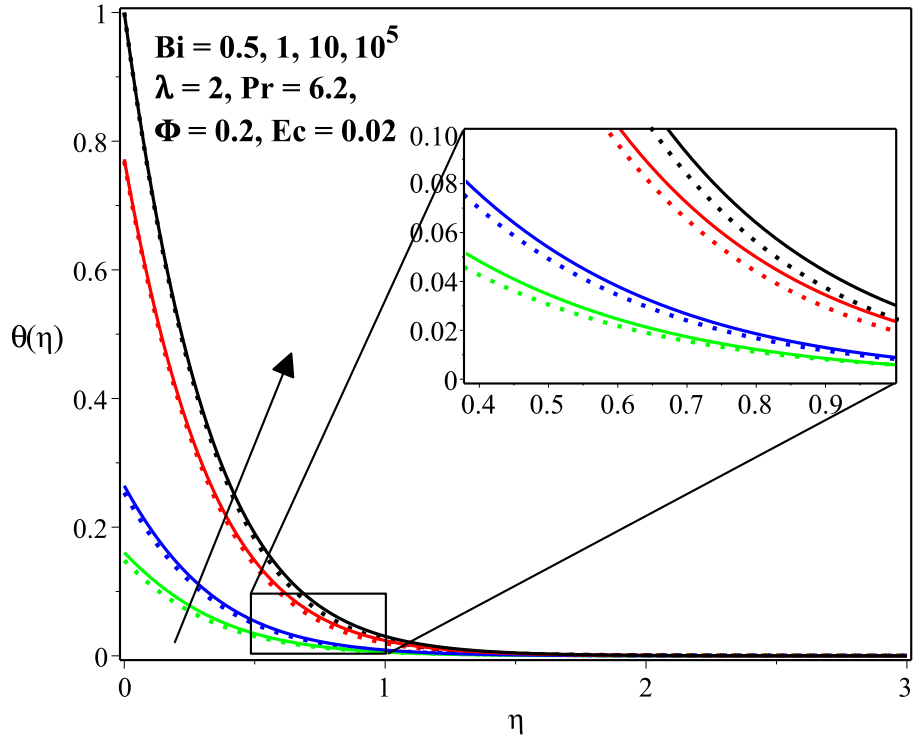

Fig. 27: Temperature profile for Biot number Bi.

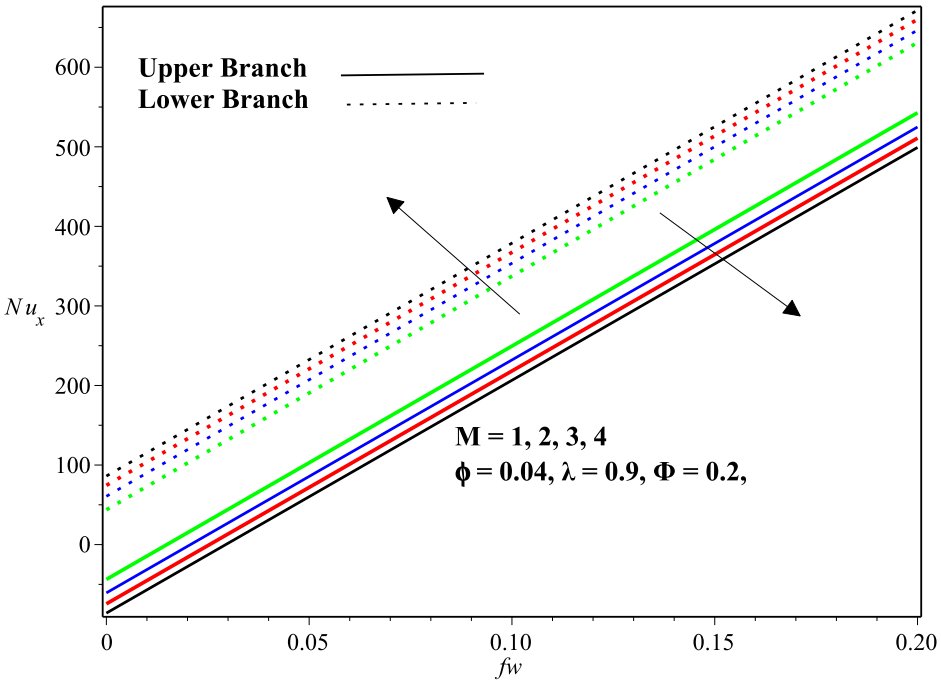

Fig. 28: Nusselt number for suction/injection f_w.

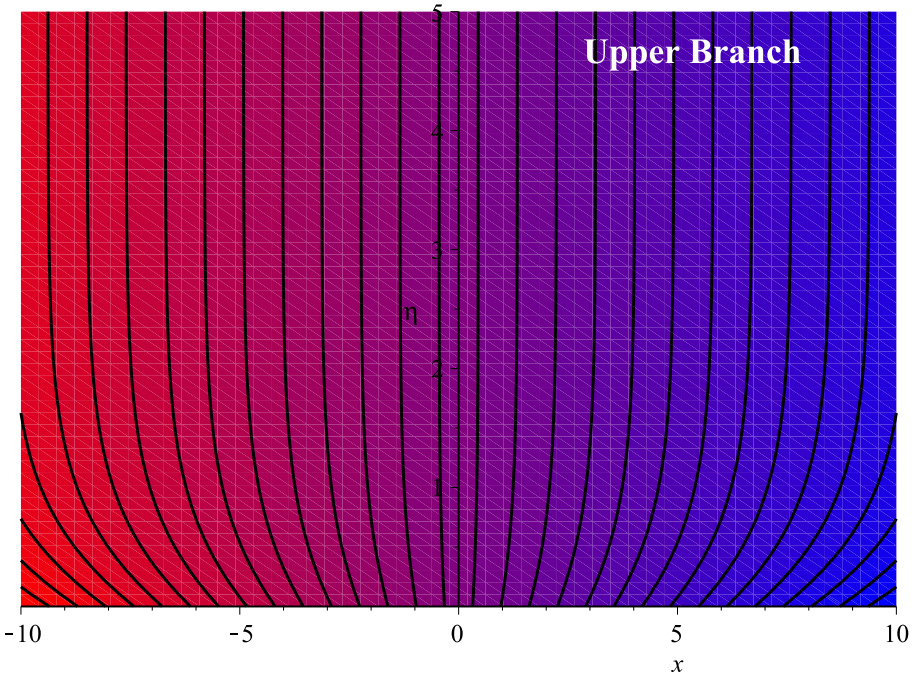

Fig. 29: Stream Lines for suction $f_w > 0$.

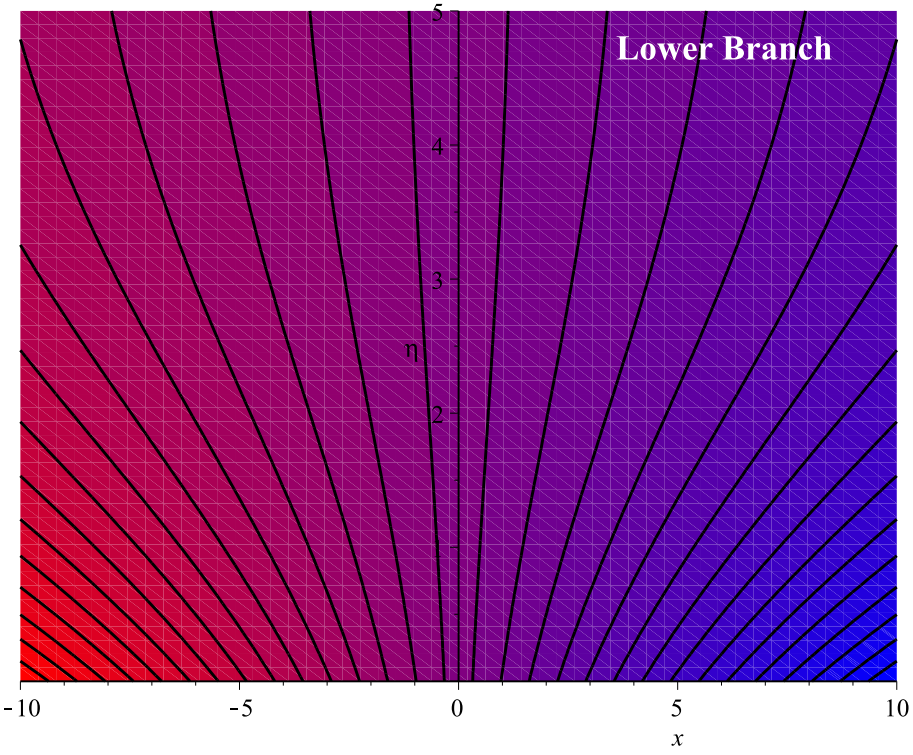

Fig. 30: Stream Lines for suction $f_w > 0$.

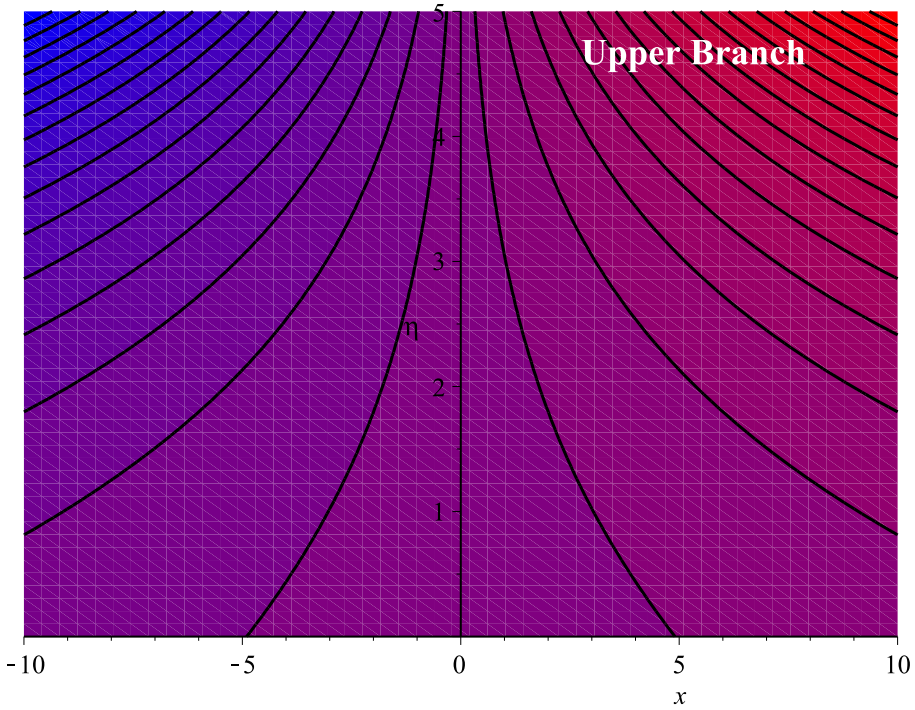

Fig. 31: Stream Lines for injection $f_w < 0$.

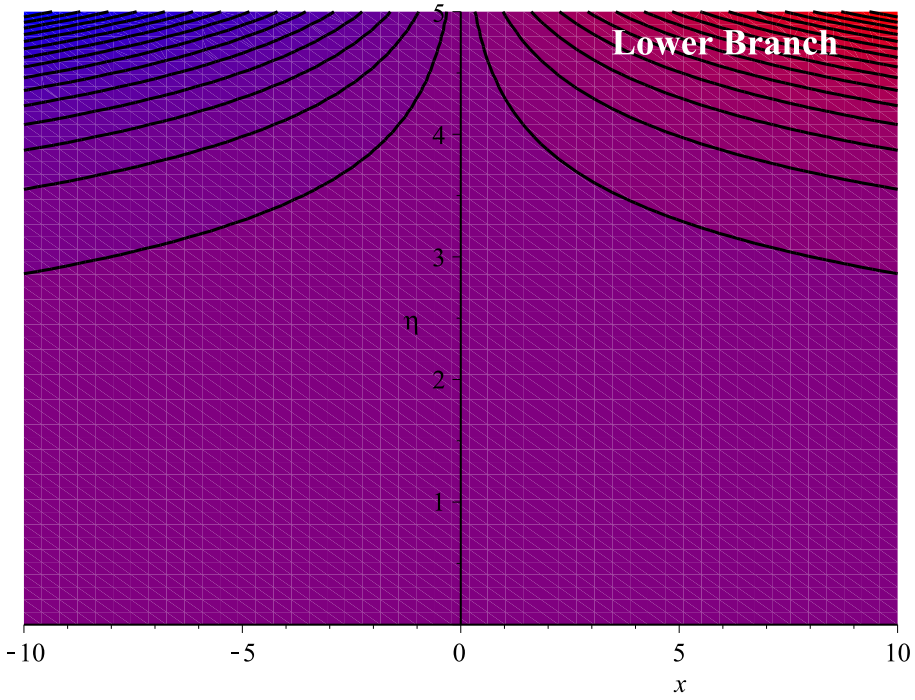

Fig. 32: Stream Lines for injection $f_w < 0$.

Chapter 5

Conclusion

This chapter sums up the analytical and graphical findings from the review and extension effort. In this chapter we discuss all of the results from the preceding two articles. Following points are noted:

- The governing PDEs are transformed to nonlinear dimensional ODEs through a similarity transformation for an exact solution.
- The dimensionless ODEs of energy and momentum produced a dual nature solution in closed form under certain conditions.
- To deal with the nanofluid, the KKL model is used and the equations are solved using well-known software Maple.
- Variation in skin friction, velocity, temperature and streamlines against suction f_w, stretching λ, porosity Φ and magnetic field M are explained and depicted in figures.
- In upper branch, magnetic M and suction f_w boost the velocity profile whereas behavior is revers in lower branch.
- The thickness of thermal boundary layer declined against rising suction f_w and stretching λ.
- Skin friction C_f rising with increasing porosity (Φ) and stretching λ for suction when $f_w > 0$ and it decreases for injection when $f_w < 0$.
- The thickness of thermal boundary layer directly varies with increasing radiation Rd, Biot number Bi and Eckert number Ec.

References

[1] Choi, SUS,. Enhancing conductivity of fluids with nanoparticles. ASME Fluid (1995) Eng Div 231:99–105.

[2] Das, SK, Choi SUS, Yu W, Pradeep T. Nanofluids: science and technology. Wiley, (2007) NJ.

[3] Cheng, Lixin. Nanofluid Heat Transfer Technologies. Recent Patents on Engineering. (2009). (3-10).

[4] Yang, Z.G. Zhang, E.A. Grulke, W.B. Anderson, G. Wu, Heat transfer properties of nanoparticle-in-fluid dispersions (nanofluids) in laminar flow, Int. J. Heat Mass Transf. 48 (6) (2005) 1107–1116.

[5] Tiwari,R.K., M.K. Das, Heat transfer augmentation in a two-sided lid-driven differentially heated square cavity utilizing nanofluids, Int. J. Heat Mass Transf. 50 (2007) (9–10) .

[6] Aminreza, N, Rashid P, Mohamed G Effect of partial slip boundary condition on the flow and heat transfer of nanofluids past stretching sheet prescribed constant wall temperature. Int J Therm Sci (2012) 1–9.

[7] Hayat, T. Hayat, M.I. Khan, M. Waqas, A. Alsaedi, M. Farooq, Numerical simulation for melting heat transfer and radiation effects in stagnation point flow of carbon-water nanofluid, Comput. Methods Appl. Mech. Engrg. (2016).

[8] Hamad, M. Analytical solution of natural convection flow of a nanofluid over a linearly stretching sheet in the presence of magnetic field. Int Commun Heat Mass Transfer (2011) 38:487–492.

[9] Yacob, NA, Ishak A, Nazar R, Pop I Boundary layer flow past a stretching/shrinking surface beneath an external uniform shear flow with a convective surface boundary condition in a nanofluid. Nanoscale Res Lett 6 (2011):1–7.

[10] Oztop, HF, Abu Nada E. Numerical study of Natural ventilation in possibly hot nanofluid filled rectangular enclosures, Int. J. Heat fluid flow, 29 (2008), 1326 - 1336.

[11] Nadeem, S. , R. Ul Haq, MHD boundary layer flow of a nanofluid passed through a porous shrinking sheet with thermal radiation, J. Aerosp. Eng. 28 (2) (2015) 04014061.

[12] Prandtl, L. Prandtl, in Verhandlungen des dritten internationalen Mathematiker-Kongresses in Heidelberg 1904, A. Krazer, ed., Teubner, Leipzig, Germany (1905), p. 484.

[13] Sakiadis, BC. Boundary-layer behavior on continuous solid surface: I. Boundary-layer equations for two-dimensional and axisymmetric flow. J AIChe, 7 (1961), 26 – 28.

[14] Erickson, L.E., Fan, L.T. and Fox, V.G. Heat and Mass Transfer on Moving Continuous Flat Plate with Suction or Injection. Industrial and Engineering Chemistry Fundamentals, 5, (1966) 19-25.

[15] Crane, L.J., Flow past a stretching plate, Z. Angew. Math. Mech., 21 (1970), 645 - 647.

[16] Gupta, PS., Gupta AS, Heat and mass transfer on a stretching sheet with suction or blowing. Can J Chem Eng 55 (1977) :744–746.

[17] Grubka, LJ, Bobba KM Heat transfer characteristics of a continuous stretching surface with variable temperature. ASME J Heat Transfer 107 (1985) :248–250.

[18] Banks, WHH, Similarity solution of the boundary layer equation for a stretching wall. J Mech Theory Appl 2 (1983) :375–392

[19] Ali, ME, On thermal boundary layer on a power law stretched surface with suction or injection. Int J Heat Mass Flow 16 (1995):280–290.

[20] Elbashbeshy, EMA, Heat transfer over a stretching surface with variable heat flux. J Phys D Phys 31 (1998) :1951–1955.

[21] Miklavcic, M., C.Y. Wang, Viscous flow due to shrinking sheet, Quart. Appl. Math., 64 (2006), 283 - 290.

[22] Wang, C Y, International Journal of Non-Linear Mechanics, 43 (2008), 377.

[23] Kumaran, V. , G. Ramanaiah, A note on the flow over a stretching sheet, Acta Mech., 116 (1996), 229 - 233.

[24] Ishak, A, Nazar R, Pop I,. Heat transfer over an unsteady stretching permeable surface with prescribed wall temperature. Nonlinear Anal Real World Appl 10 (2009) :2909–2913.

[25] Khan, W.A., I. Pop, Boundary layer flow of a nanofluid past a stretching sheet, Int. J. Heat Mass Transfer 53 (2010) 2477 – 2483.

[26] wahed, Abdel, M..,. An exact solution of boundary layer flow over a moving surface embedded into a nanofluid in the presence of magnetic field and suction/injection. Heat and Mass Transfer. 50. (2013) 57–64.

[27] Koo, Junemo and Kleinstreuer, Clement. ,. A new thermal conductivity model for nanofluids . Journal of Nanoparticle Research. 7.(2005) 324-324.

[28] Li, J.Computational analysis of nanofluid flow in microchannels with applications to micro-heat sinks and bio-MEMS[Ph.D thesis] Raleigh,NC,UnitedStates: NC State University; (2008).

[29] Hosseini, S.R., M. Sheikholeslami, M. Ghasemian, D.D. Ganji, Nanofluid heat transfer analysis in a microchannel heat sink (MCHS) under the effect of magnetic field by means of KKL model, Powder Technology, 324, (2018), 36-47.

[30] Ali, Sulaiman Alsagri, Rasoul Moradi, Application of KKL model in studying of nanofluid heat transfer between two rotary tubes, Case Studies in Thermal Engineering,14, (2019), 100478.

[31] Pourmehran, M. Rahimi-Gorji, M. Hatami, S.A.R. Sahebi, G. Domairry, Numerical optimization of microchannel heat sink (MCHS) performance cooled by KKL based nanofluids in saturated porous medium, Journal of the Taiwan Institute of Chemical Engineers, 55, (2015), 49-68.

[32] Kandelousi, Mohsen Sheikholeslami. KKL correlation for simulation of nanofluid flow and heat transfer in a permeable channel. Physics Letters A 378 (2014): 3331-3339.

[33] Khan,W.A., I. Pop, Heat Transfer Near Stretching Surface in Porous Medium Using Thermal Non-Equilibrium Model, AIAA J. Thermo-phys. Heat Transfer 26 (2012), 681 – 685.

[34] Khan, Z.H., M. Qasim, Rizwan ul Haq, Qasem M.Al-Mdallal, Closed dual nature fluid flow and heat transfer solutions via a porous media stretch/shrink sheet, Chinese Journal of Physics, 55 (2017), 1284 - 1293.

[35] Haq, Rizwan ul, Raza, Ali, Algehyne, Ebrahem and Tlili, Iskander. Dual nature study of convective heat transfer of nanofluid flow over a shrinking surface in a porous medium. International Communications in Heat and Mass Transfer. 114. (2020) 104583. 10.1016.

[36] Haq, Rizwan Ul, T. Sajjad, M.Z. Ullah, A.S. Alshomrani, Iskander Tlili, Dual nature solutions of water-based carbon nanotubes along a shrinking Surface with heat radiation and viscous dissipation, International Communications in Heat and Mass Transfer, 119, (2020), 104938.

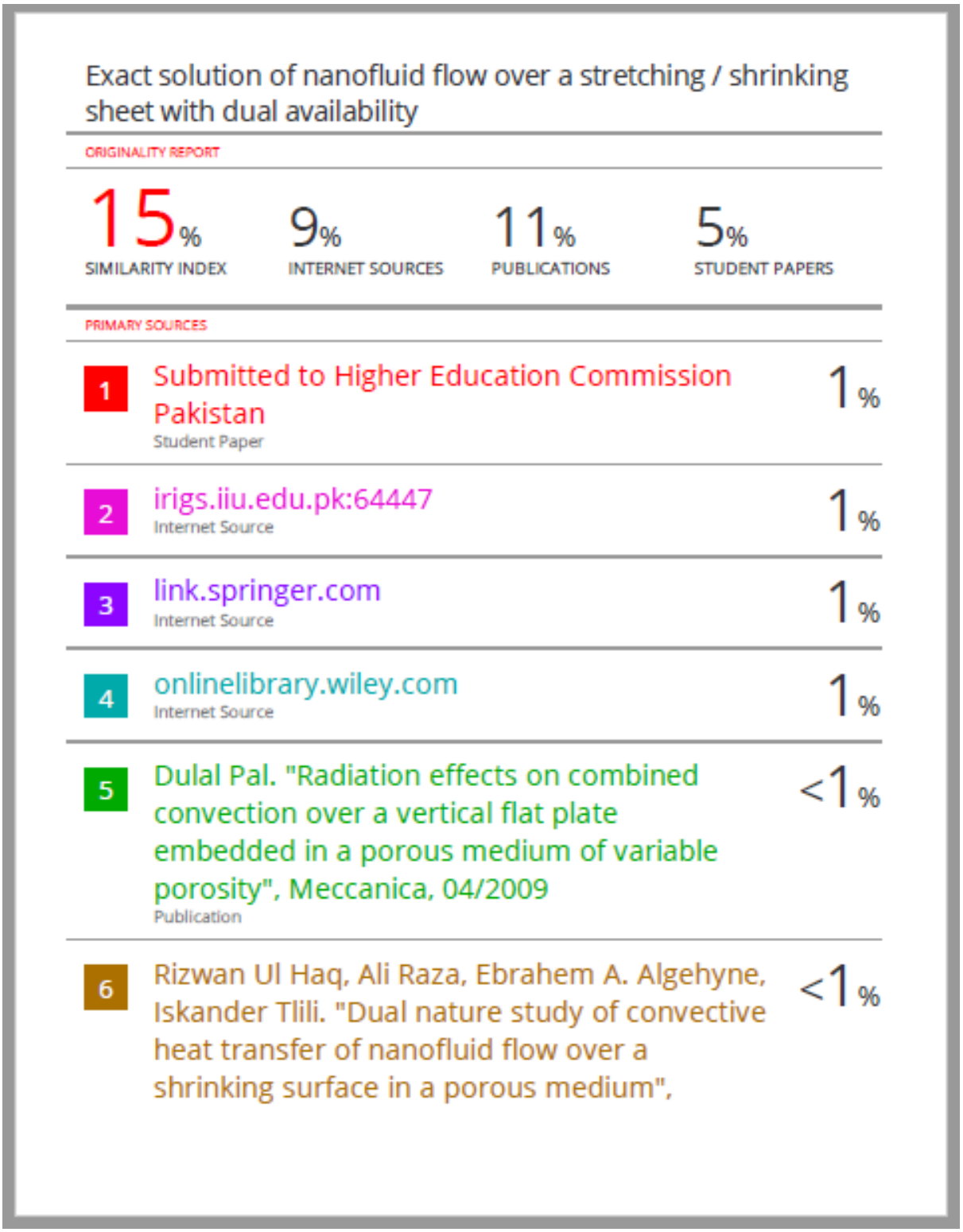

Exact solution of nanofluid flow over a stretching / shrinking sheet with dual availability

ORIGINALITY REPORT

15%	9%	11%	5%
SIMILARITY INDEX	INTERNET SOURCES	PUBLICATIONS	STUDENT PAPERS

PRIMARY SOURCES

1	Submitted to Higher Education Commission Pakistan Student Paper	1%
2	irigs.iiu.edu.pk:64447 Internet Source	1%
3	link.springer.com Internet Source	1%
4	onlinelibrary.wiley.com Internet Source	1%
5	Dulal Pal. "Radiation effects on combined convection over a vertical flat plate embedded in a porous medium of variable porosity", Meccanica, 04/2009 Publication	<1%
6	Rizwan Ul Haq, Ali Raza, Ebrahem A. Algehyne, Iskander Tlili. "Dual nature study of convective heat transfer of nanofluid flow over a shrinking surface in a porous medium",	<1%